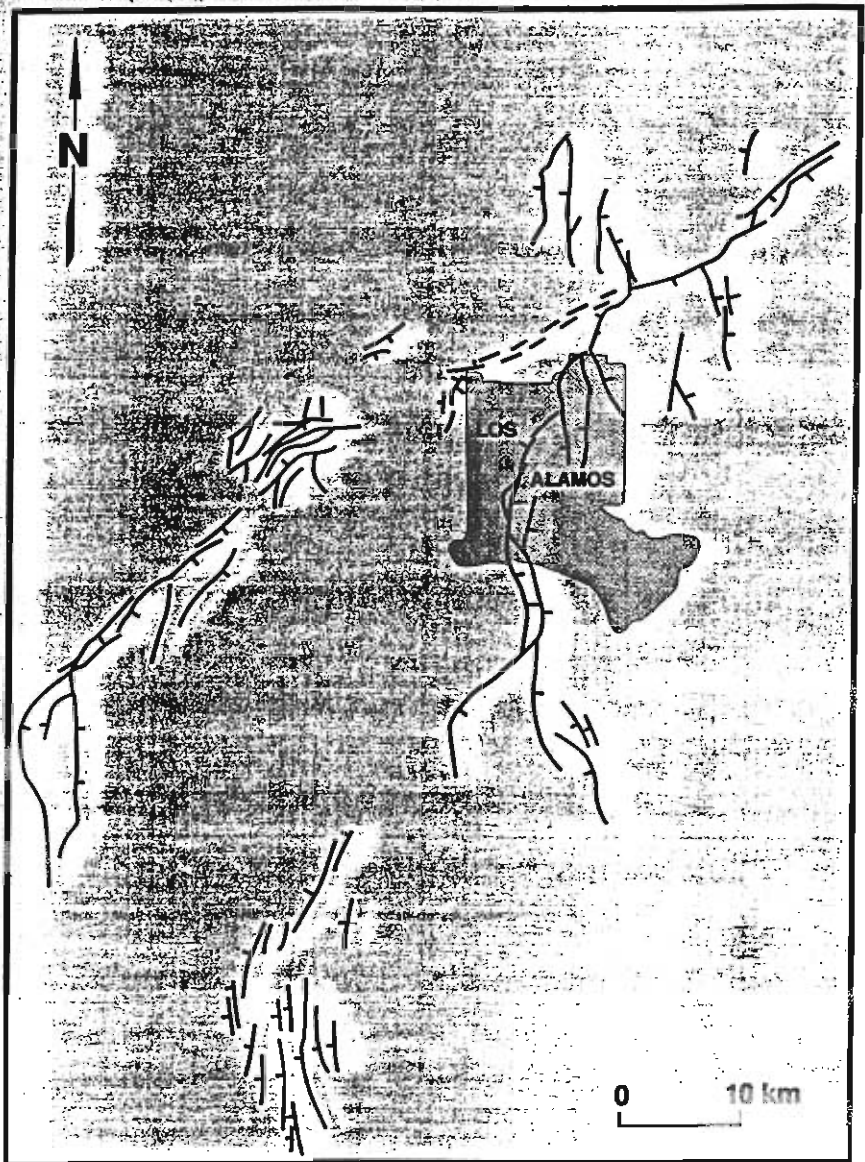


LA-13522-MS

Approved for public release;
distribution is unlimited.

2.4

*Stratigraphy and Geologic Structure
at the Chemical and Metallurgy (CMR)
Building, Technical Area 3,
Los Alamos National Laboratory*



Los Alamos
NATIONAL LABORATORY

*Los Alamos National Laboratory is operated by the University of California
for the United States Department of Energy under contract W-7405-ENG-36.*

*Stratigraphy and Geologic Structure
at the Chemical and Metallurgy (CMR)
Building, Technical Area 3,
Los Alamos National Laboratory*

*Donathan Krier
Florie Caporuscio
Jamie Gardner
Alexis Lavine*



Prepared by Lanny Piotrowski, Group EES-1

An Affirmative Action/Equal Opportunity Employer

This report was prepared as an account of work sponsored by an agency of the United States Government. Neither The Regents of the University of California, the United States Government nor any agency thereof, nor any of their employees, makes any warranty, express or implied, or assumes any legal liability or responsibility for the accuracy, completeness, or usefulness of any information, apparatus, product, or process disclosed, or represents that its use would not infringe privately owned rights. Reference herein to any specific commercial product, process, or service by trade name, trademark, manufacturer, or otherwise, does not necessarily constitute or imply its endorsement, recommendation, or favoring by The Regents of the University of California, the United States Government, or any agency thereof. The views and opinions of authors expressed herein do not necessarily state or reflect those of The Regents of the University of California, the United States Government, or any agency thereof. Los Alamos National Laboratory strongly supports academic freedom and a researcher's right to publish; as an institution, however, the Laboratory does not endorse the viewpoint of a publication or guarantee its technical correctness.

**STRATIGRAPHY AND GEOLOGIC STRUCTURE AT THE CHEMISTRY AND
METALLURGY RESEARCH (CMR) BUILDING, TECHNICAL AREA 3,
LOS ALAMOS NATIONAL LABORATORY, NEW MEXICO**

by

Donathon Krier, Florie Caporuscio, Jamie Gardner, and Alexis Lavine

ABSTRACT

Nine shallow (<70 ft), closely spaced core holes were continuously cored in the upper units of the 1.22 Ma Tshirege Member of the Bandelier Tuff at Technical Area (TA)-3 of the Los Alamos National Laboratory. The goal of the investigation was to identify faults that may have potential for earthquake-induced surface rupture at the site of the Chemistry and Metallurgy Research (CMR) building, a sensitive Laboratory facility that houses nuclear materials research functions. The holes were located from 25 ft to 115 ft from the building perimeter. Careful mapping of lithologic sequences in cores, supplemented with focused sampling for geochemical analyses, yielded high confidence in the accuracy of delineating buried contacts within the Tshirege Member. Geologic analysis and investigation of the trends of surfaces interpolated from contacts in the core holes using commercially available software helped infer minor faulting in the strata beneath the building. Results show that gently north-northeast-dipping beds underlie the CMR building. The tilted beds are faulted by two small, closely spaced, parallel reverse faults with a combined vertical separation of approximately 8 ft. The faults are inferred from lithologically and geochemically repeated sections of core at about 55-ft depth in hole SHB-CMR-6. The data from nearby core holes SHB-CMR-2 and SHB-CMR-3 permit the extension of the faults, albeit with decreasing separation, toward the southwest beneath the CMR building. The fault trend is consistent with mapped lineaments from aerial photography and with nearby mapped structure, but direct evidence of the faults' orientations is lacking. No other faults were detected beneath the CMR building by this drilling and analysis method, which can detect faults with greater than about 2 ft separation.

I. INTRODUCTION

Previous studies have shown that the major, potentially active faults that may affect Los Alamos National Laboratory (LANL) are the Pajarito, Rendija Canyon, and Guaje Mountain fault zones (Figure 1a) (Dransfield and Gardner, 1985; Gardner and House, 1987; Wong et al., 1995). These fault zones are commonly taken to constitute the Pajarito Fault System (e.g., Gardner and House, 1987), which defines the local active boundary of deformation of the Rio Grande Rift, a major tectonic feature of the North American continent (Gardner and Goff, 1984). How the faults of this system may physically connect or kinematically interact has important bearing on seismic hazards issues at Los Alamos but is subject to debate and is the focus of ongoing studies. The southern end of the Rendija Canyon fault was inferred to pass through or near Technical Area (TA)-55 by Wong et al. (1995); however, detailed work by Gardner et al. (1998) showed that the otherwise north-south trending fault does not pass through

TA-55, but may instead pass through TA-3 as multiple southwest-trending splays. Additionally, aerial photolineaments that may represent southwest-trending splays of the Rendija Canyon fault and kinematic interactions with the Pajarito fault zone farther west appear to converge on TA-3. Building SM-29, the Chemistry and Metallurgy Research (CMR) building, is located coincident with one of the southwest-trending photolineaments and along the zone of other southwest-trending splays that may represent an extension of the Rendija Canyon fault (Gardner, 1998, personal communication). The lineament is located on the northern half of the CMR building footprint and trends southwest; hence, exploratory core hole locations were concentrated on the southwest, northwest, and northeast areas around the building.

As part of the LANL Seismic Hazards Program, nine core holes were drilled around the perimeter of the CMR building to obtain information on the presence or absence of near-surface faults (Figure 1b). This work is part of a broader program of geoscientific efforts that seek to quantify probabilistic seismic hazards, including ground motion and surface rupture, at LANL. The objective of the drilling program at the CMR building was to drill to intercept stratigraphic markers within the Bandelier Tuff and evaluate

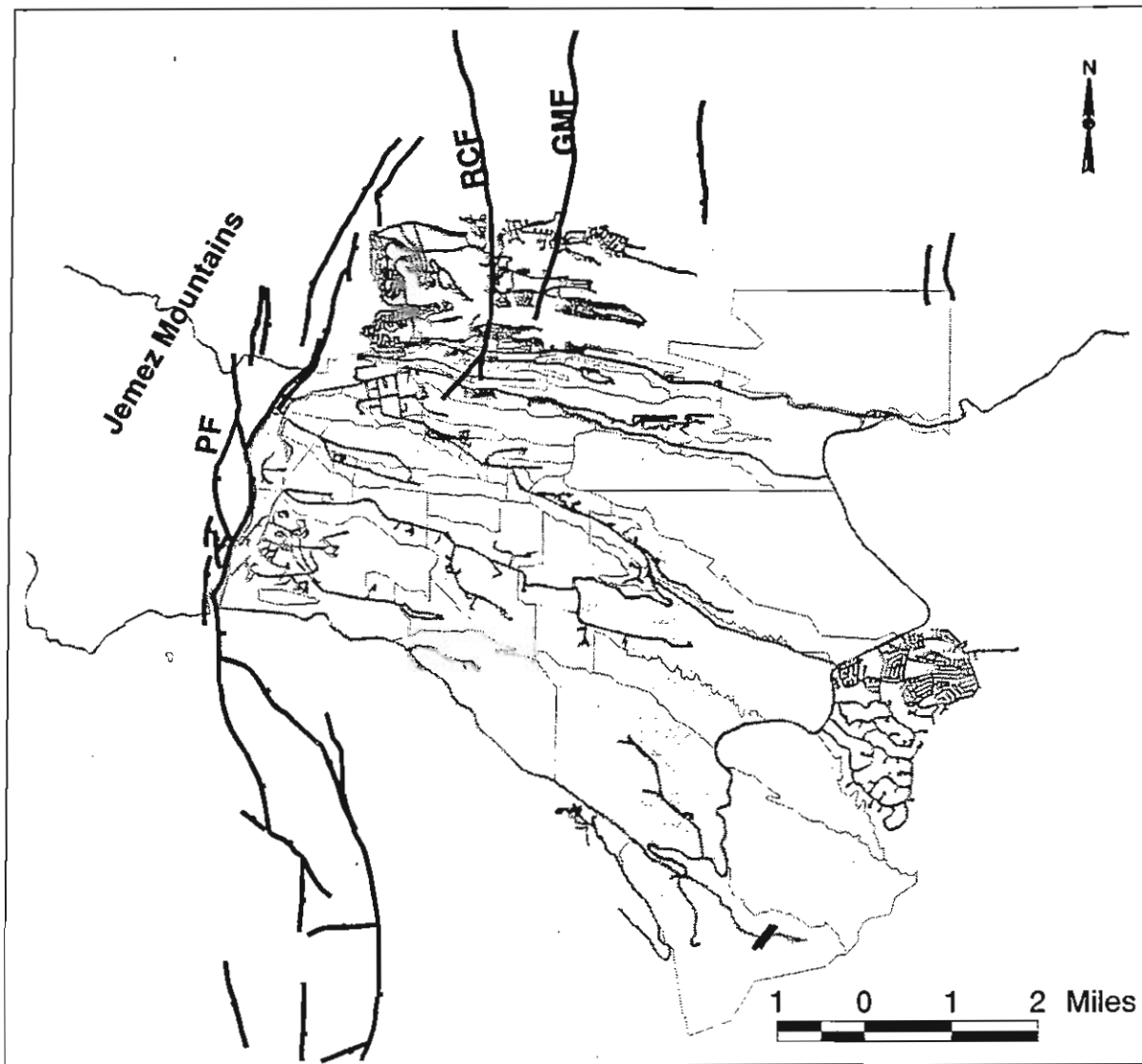


Figure 1a. Map showing the area of Los Alamos National Laboratory (shaded gray) and faults of the Pajarito Fault System (thick lines with bar on downthrown side): PF = Pajarito Fault, RCF = Rendija Canyon Fault, GMF = Guaje Mountain Fault.

any measurable stratigraphic separation (“offset”) between drill sites caused by faulting in the 1.22 Ma Tshirege Member of the Bandelier Tuff (Izett and Obradovich, 1994). The stratigraphic markers included contacts between flow units and phenocryst-rich layers (surge beds) within the Tshirege Member. Geologic cores removed from the holes were used to define and correlate the stratigraphic sequence at each drillhole to aid in identifying geologic structures that might impact the building’s foundation and structural stability in the future. In addition to risk posed by seismic ground motion, near-surface faults may have the potential for surface rupture, which could affect the integrity of building foundations and systems in the event of large earthquakes.

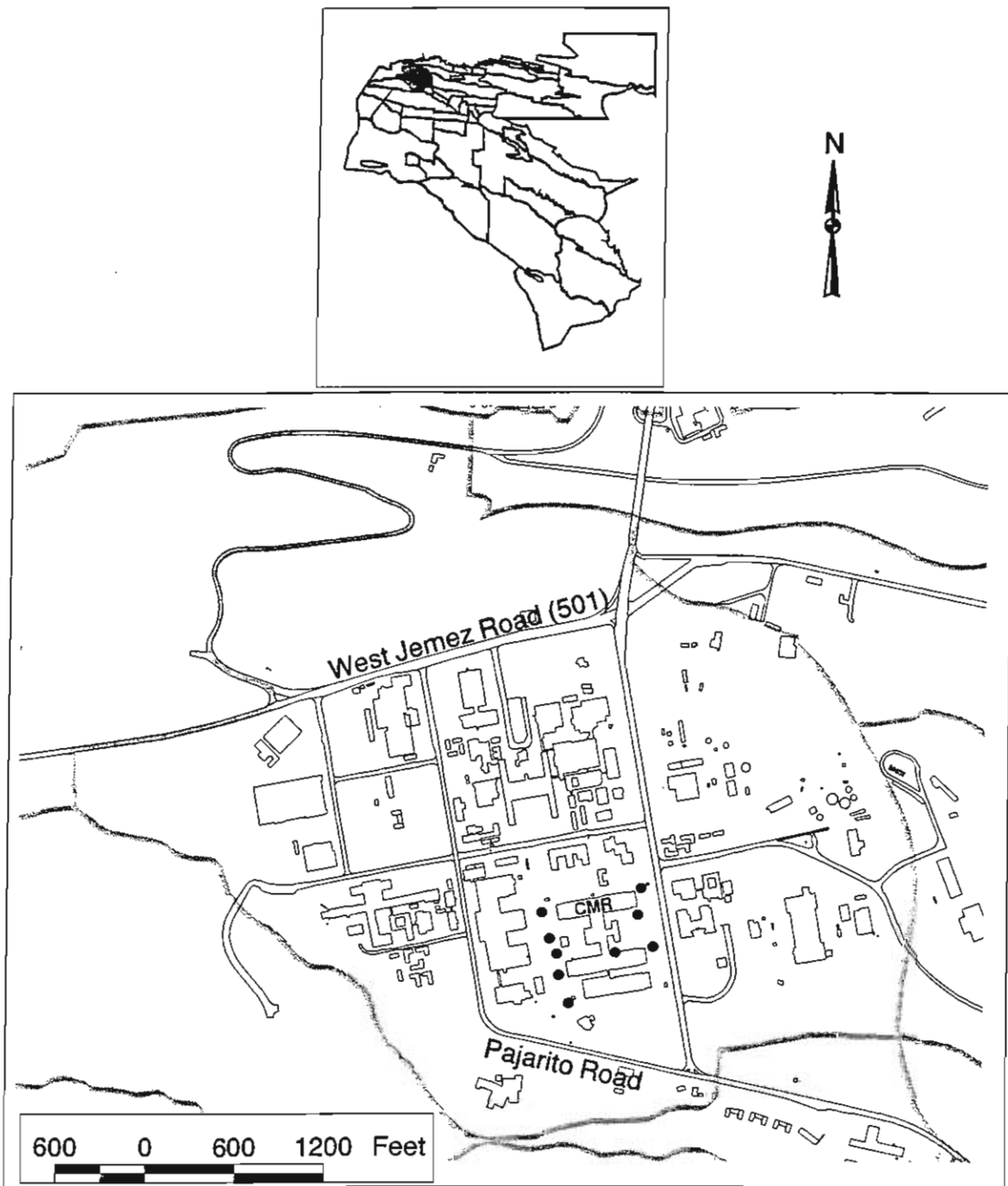


Figure 1b. The upper map shows the outline of Los Alamos National Laboratory with Technical Areas (TA) outlined in black. TA-3 is shaded gray. The lower map shows TA-3 and the locations of the core holes (black dots) around the CMR building.

The core hole locations in relation to the outline of the CMR building are shown in Figure 1c. Core hole designations and coordinates are listed in Table 1. Note that core hole SHB-CMR-9, located 200 ft west of SHB-CMR-7 and planned to be drilled last, was not drilled because of the small amount of additional data expected from that location. The core holes were arrayed around the CMR building and offset from exterior walls from 25 to 115 ft. Final locations were selected to avoid buried electrical utilities, water pipelines, radioactive waste pipelines, and communication lines. Utilities were located using as-built drawings, visual inspections, and induced radio-frequency detection (Metratech 810 detector). Radio-frequency detectors are typically used by municipalities for locating shallowly buried utility lines.

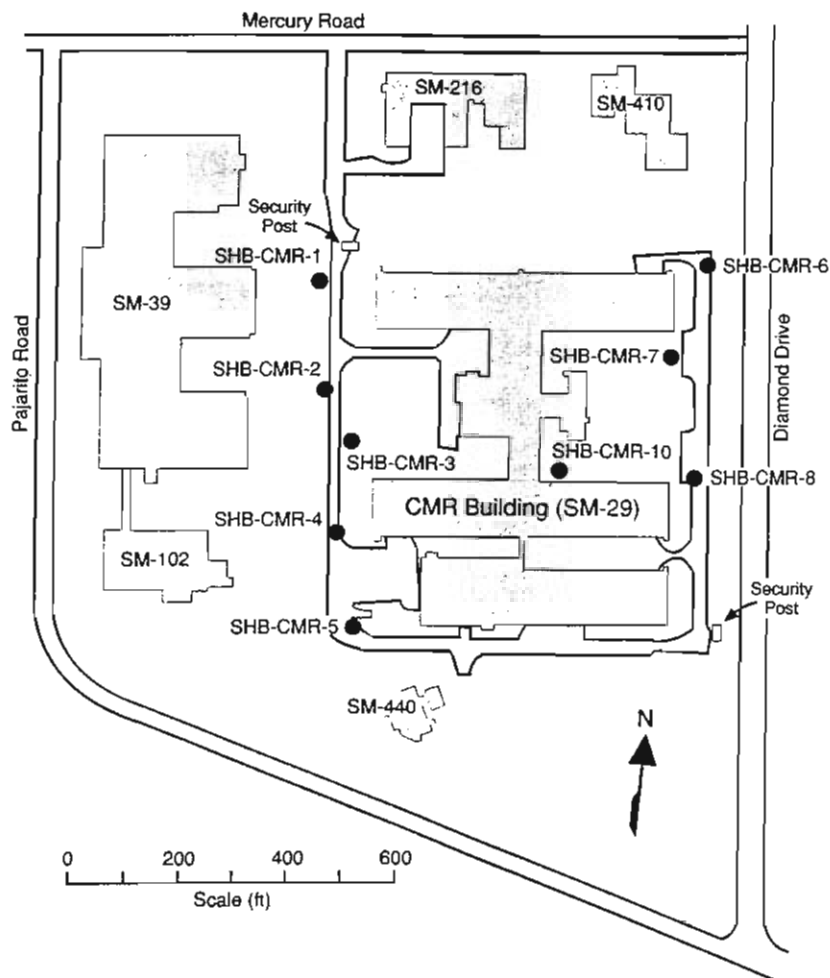


Figure 1c. Map of the nine SHB-CMR core holes and selected buildings at TA-3.

II. METHODS

Drilling and coring operations took place from May 13 through May 21, 1998. The holes were augered in 2.5-ft core lengths using a hollow-stem auger with a split-spoon barrel and wireline retrieval system powered by a CME Model 750 drill rig. The core diameter was 3.5 inches. A total of 517.5 ft was drilled in 7 days with 98% core recovery. Daily operations at the rig were supported by a crew of three drillers, two geologists, a safety oversight professional, and a security escort. Each core was screened before logging using a hand-held organic vapor analyzer and radiation monitors for alpha (Ludlum Model 139) and beta-gamma (Eberline ESP-1) detection. None of the cores showed signs of organic chemicals or radioactive contamination. The excellent core recovery is attributed to the drillers' familiarity with the rock type, careful drilling with emphasis on core recovery, and a shallow target

Table 1. Coordinates for the nine CMR core holes. State Plane Coordinate System, New Mexico Central Zone, 1983 North American Datum.

Core hole	Northing (ft)	Easting (ft)	Ground Elev. (ft)
SHB-CMR-1	1772678.60	1618571.21	7402.23
SHB-CMR-2	1772502.63	1618622.93	7399.77
SHB-CMR-3	1772403.05	1618671.66	7398.61
SHB-CMR-4	1772262.73	1618683.58	7398.35
SHB-CMR-5	1772075.21	1618750.74	7397.46
SHB-CMR-6	1772823.24	1619258.44	7392.16
SHB-CMR-7	1772670.59	1619211.22	7394.91
SHB-CMR-8	1772450.24	1619307.99	7392.72
SHB-CMR-10	1772412.72	1619061.52	7398.41

depth (<70 ft) for each hole. Lithologic logs were prepared for each hole at the drill sites immediately upon retrieval of the core and were supplemented with later detailed examination of key intervals at LANL's Environmental Restoration Project Field Support Facility where the cores are archived. Cores were marked and boxed at the drill sites using a procedure designed by Goff (1986) as guidance. The logs include descriptions of lithology, fractures, fracture fill, texture, and mineralogy, and the locations of samples taken for chemical analyses. Although core recovery was excellent, the effects of drilling, the often poor sample induration, and the consequences of handling reduced most nonwelded to partly welded intervals of core to loose powder when transferred to archive boxes. Consequently, many primary textures that were observable in the core barrel did not survive transfer to the core box.

Major and trace elements were analyzed for 64 bulk-rock samples using an automated Rigaku wavelength-dispersive x-ray fluorescence (XRF) spectrometer. Samples were first crushed and homogenized in 15- to 20-g portions in a tungsten-carbide shatterbox in accordance with Yucca Mountain Project procedure LANL-EES-DP-130 — Geologic Sample Preparation. Sample splits were heated at 110°C for 4 h, and then allowed to equilibrate with ambient atmosphere for 12 h. One gram splits were fused at 1100°C with 9 grams of lithium tetraborate flux to obtain the fusion disks. Additional one-gram splits were heated at 1000°C to obtain the loss-on-ignition (LOI) measurements. Elemental concentrations were calculated by comparing x-ray intensities for the samples to those for 21 standards of known composition. A fundamental parameters program was used for matrix corrections (Criss, 1980). The XRF method employed calculates the concentrations of ten compounds (SiO₂, TiO₂, Al₂O₃, Fe₂O₃, MnO, MgO, CaO, Na₂O, K₂O, P₂O₅), ten minor elements (V, Cr, Ni, Zn, Rb, Sr, Y, Zr, Nb, Ba), and LOI. As discussed below, the compositional data were used to confirm and (or) tighten control on elevations of the geologic contacts between stratigraphic units of the Tshirege Member of the Bandelier Tuff.

III. STRATIGRAPHY AND NOMENCLATURE

The stratigraphic units of the Bandelier Tuff used as markers in this drilling program are largely based on those defined by Broxton and Reneau (1995), with the addition of a transitional Unit 3t (Broxton and Gardner, 1998, personal communication), which was described by Warren et al. (1998) and encountered in earlier drilling by the Seismic Hazards Program (Krier et al., 1998). The Bandelier Tuff (Figure 2) is dominantly composed of a complex sequence of nonwelded to welded ignimbrites that were erupted from the Valles-Toledo caldera complex (Griggs, 1964; Smith and Bailey, 1966; Smith et al., 1970; Gardner et al., 1986). Beneath the Laboratory, the Bandelier Tuff consists of two members: the lower Otowi Member (1.61 Ma) and the upper Tshirege Member (1.22 Ma) (Izett and Obradovich, 1994), separated by volcanoclastic rocks and tuffs of the Cerro Toledo interval (Smith et al., 1970;

Heiken et al., 1986; Broxton and Reneau, 1995, Lavine et al., 1997). At the drill site, the Tshirege Member consists of at least four mappable units (Units 1 through 4). A thin wedge of clayey alluvium and some construction fill overlie Unit 4 and form the surface deposits at the drill site, although Unit 4 outcrops at the surface just west of the CMR building. The nine core holes at the CMR building were designed to penetrate Unit 4 and identify the contacts with underlying Units 3t and 3. Table 2 lists the core holes, total depths, and contact depths and elevations resulting from the drilling and analysis.

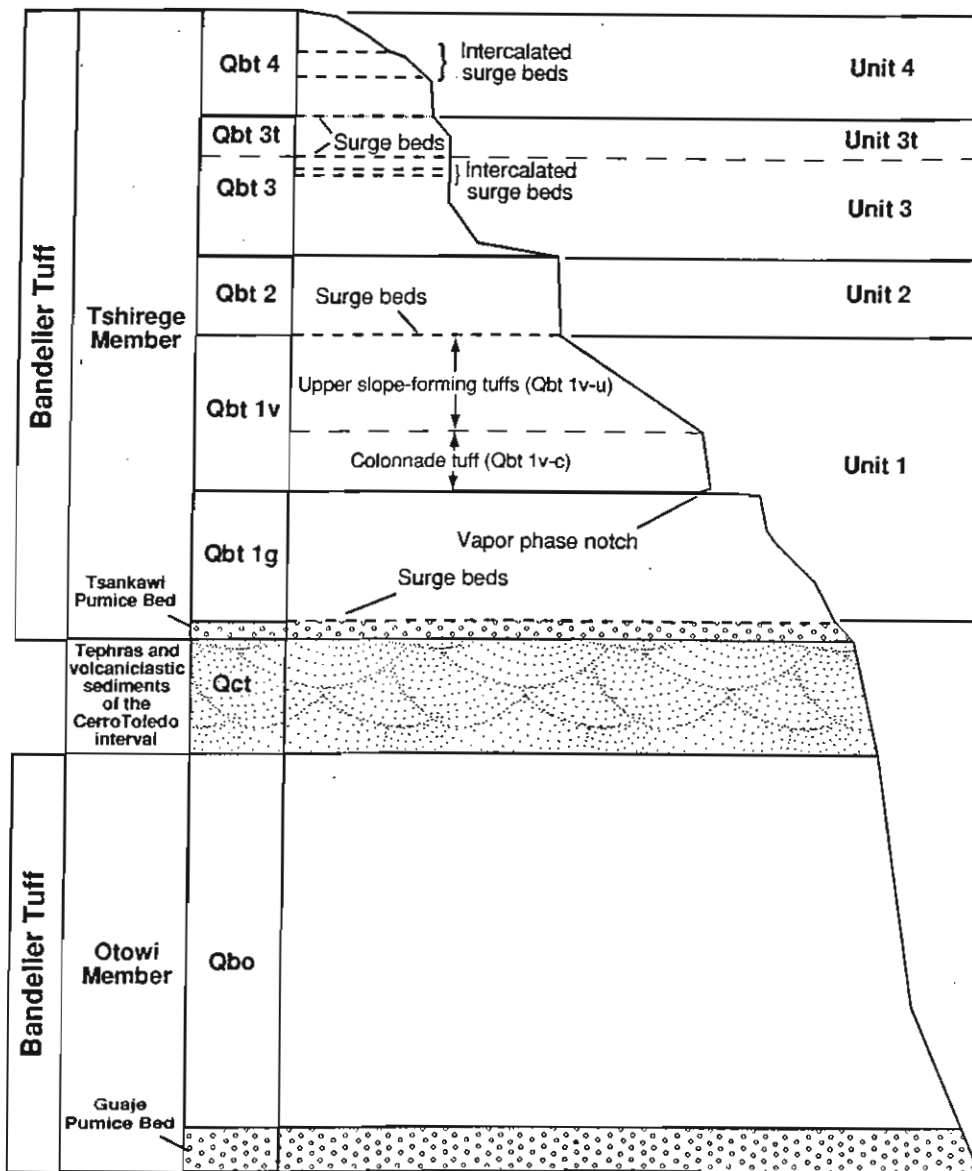


Figure 2. Composite stratigraphy of the Bandelier Tuff on the Pajarito Plateau, modified from Broxton and Reneau (1995). At any given locality, units can pinch out or swell in thickness. Note the surge beds at various unit boundaries and within Unit 4 and upper Unit 3. The SHB-CMR core holes penetrated Units 4, 3t, and 3 only.

IV. LITHOLOGIC DESCRIPTIONS

Field descriptions of the CMR cores were supplemented with binocular microscope examinations of cores at the Field Support Facility. Except for differences in texture and induration because of variations in welding (as qualitatively determined by degree of pumice flattening), the lithologic descriptions of Units 3, 3t, and 4 are consistent from hole to hole. Specific characteristics of the degree of welding,

Table 2. Core hole designations, total depths, and significant stratigraphic contact depths in the nine SHB-CMR core holes.

Borehole	Top Elevation (ft)	Total Depth (ft) (elevation)	Post-Bandelier Sediment (ft)	Surge Intervals (ft)	Units 4/3t		Units 3t/3		Unit 3t Thickness (ft)
					Contact Depth (ft)	Contact Elev. (ft)	Contact Depth (ft)	Contact Elev. (ft)	
SHB-CMR-1	7402.2	67.5 (7334.7)	0.7	47.0-47.2 57.1-57.3	47.2	7355.0	57.3	7344.9	10.1
SHB-CMR-2	7399.8	62.5 (7337.3)	1.4	42.0-42.4 49.9-50.2	42.4	7357.4	50.2	7349.6	7.8
SHB-CMR-3	7398.6	55.0 (7343.6)	0.0	50.3-52.2 37.2-37.5	39.1	7359.5	45.2	7353.4	6.1
SHB-CMR-4	7398.4	52.5 (7346.0)	1.4	38.2-39.1 36.0-36.2	36.2	7362.2	43.5	7354.9	7.3
SHB-CMR-5	7397.5	52.5 (7345.0)	0.0	38.0-38.1 39.0-39.1	33.5	7364.0	39.1	7358.4	5.6
SHB-CMR-6	7392.2	57.5 (7334.7)	2.2	47.2-47.5 50.6-50.7 53.0-53.1	47.5	7344.7	50.0	7342.2	2.5
SHB-CMR-7	7394.9	57.5 (7337.4)	0.8	45.3-46.5 52.2-52.5	46.5	7348.4	57.8	7334.4**	6.0
SHB-CMR-8	7392.7	52.5 (7340.2)	1.4	40.3-42.5 44.7-45.0	42.5	7350.2	45.0	7347.7	2.5
SHB-CMR-10	7398.4	60.0 (7338.4)	~20*	42.0-42.3 49.2-50.0 52.0-53.1 53.6-53.7 54.7-55.0	42.3	7356.1	50.0	7348.4	7.7

*Includes some fill, and tuff disturbed by building construction.

**Multiple Unit 3t/3 contacts reflect the stratigraphic repetition caused by two inferred reverse faults.

The Unit 3t/Unit 3 contact depth (57.8 ft) below the total depth of hole SHB-CMR-6 is geologically inferred.

stratigraphic assignments, and surge locations for each core hole are summarized in Figure 3. Color references follow the descriptions shown in the Rock-Color Chart (Geological Society of America, 1980). The units are described below from oldest to youngest in stratigraphic position. No water-producing intervals were encountered during this drilling, although moist-to-wet sediments and tuff are present directly beneath landscaped areas.

Unit 3 Lithologic Description

Unit 3 consists of a nonwelded to moderately welded, pumice-poor, phenocryst-rich, devitrified ignimbrite. During drilling operations, the entire thickness was not penetrated; rather, a short interval (5.0 to 13.4 ft) of Unit 3 was penetrated and sampled to confirm the contact between Unit 3 and Unit 3t by visual and geochemical means. This unit is nonwelded at the top but grades downward to moderately welded rock over a short interval (5 to 10 ft).

Phenocrysts in Unit 3 are abundant at 25 to 35 volume percent (vol %), with quartz and sanidine in subequal amounts and with lesser plagioclase. Phenocrysts are larger (averaging 4 mm) and from 30% to 50% more abundant than in Unit 4. Whole quartz crystals are bipyramidal (characteristic of this ignimbrite), approximately 4 mm on an edge, and make up 15 to 17 vol % of the tuff. However, more than half the population of all crystal types consists of broken fragments. Sanidines are similar in size (4 mm) and abundance (approximately 15 vol %), and exhibit a blue chatoyance in sunlight. The rare and small (<1-mm) mafic phenocrysts comprise only 1 to 2 vol % of the tuff and are mostly biotite.

Pumices in the ignimbrite range from 4 to 7 vol % and are fully inflated toward the top of the unit, exhibiting primary tube structures. With increasing welding, the tube structures are deformed and flattened. All pumices are devitrified, and colors are primarily dark gray or light brown. The pumices range in size from 5 mm to over 7 cm.

The matrix of Unit 3 is made up of devitrified glass shards, crystal fragments, and very small pumice fragments. Matrix color ranges from pinkish gray to pale gray and the matrix makes up approximately 65 vol % of the ash flow. Lithics are rare and make up less than 1 vol % of the tuff.

Crystal-rich surge horizons are not widespread in our limited core from Unit 3, but three intercalated surges are present in upper Unit 3 in core hole SHB-CMR-10, one in core hole SHB-CMR-6, and another thick surge or surge-like deposit in Unit 3 is present in SHB-CMR-2. The beds are light gray in color, medium-to-coarse grained, and massive-to-laminar bedded, loosely consolidated sands. In SHB-CMR-10, the two lower surges (53.6 to 53.7 ft and 54.7 to 55.0 ft) are distinct and separated by a thin nonwelded tuff. The contacts of the upper surge (52.0 to 53.1 ft) are very gradational because of fine ash being progressively depleted in the 2-to-3-ft interval located directly above and below the surge. Hole SHB-CMR-2 contains an approximately 2-ft-thick surge bed at the top of Unit 3.

Unit 3t Lithologic Description

Unit 3t has three differences from Unit 3 that are readily observable in hand sample. The most obvious variation is decreased phenocryst percentage, which was used as the major criterion in the field to indicate the presence of Unit 3t. This unit has a phenocryst volume of 18% to 25%, transitional between Units 3 (25% to 35%) and 4 (8% to 15%). The second difference is the degree of welding. Unit 3t is often first encountered in the core as moderately to densely welded tuff. Even when the first Unit 3t

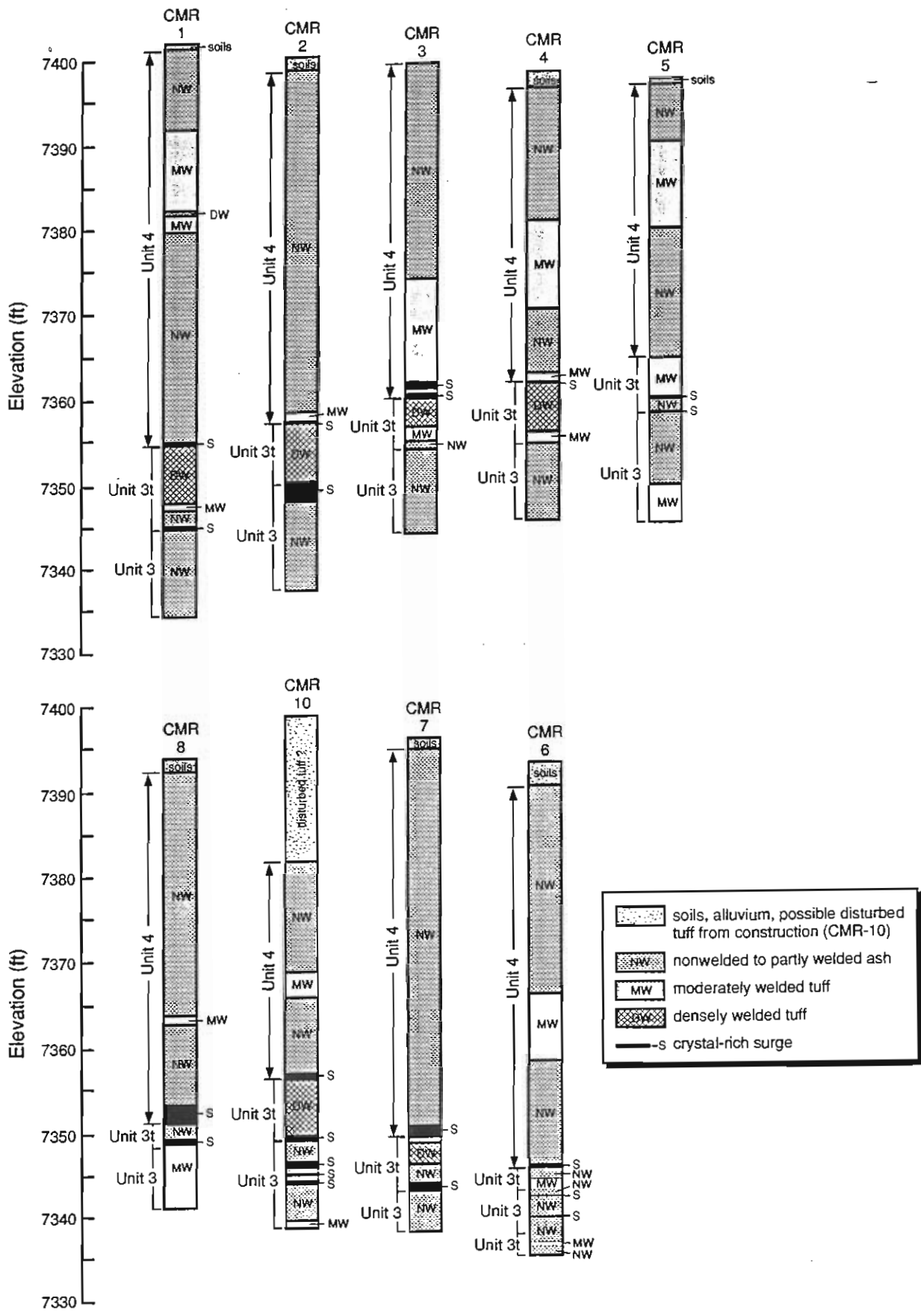


Figure 3. Stratigraphic columns, welding characteristics, and surge locations for the nine SHB-CMR core holes.

material is observed to be nonwelded ash, it rapidly becomes welded over an interval of a few feet. The final variation observed sporadically in Unit 3t is the presence of large, light gray flattened pumices. These pumices can extend across the sampled core and mimic white banding in the tuff. The pumices are both deformed and slightly altered. Unit 3t varies in thickness from 0.9 to 10.1 ft and averages 5 ft at the CMR site.

Crystal-rich surge beds, depleted in fine ash, were identified at the base of Unit 3t in six core holes (SHB-CMR-1, -2, -5, -7, -8, -10). These beds, primarily composed of sand-sized quartz and feldspar crystals (60 to 95 vol %), range in thickness from 0.1 to 0.8 ft. The base of Unit 3t in SHB-CMR-5 is marked only by a thin, horizontal sandy parting in the core.

Unit 4 Lithologic Description

Unit 4 is a nonwelded to densely welded, moderately pumice-rich, and phenocryst-poor to moderately phenocryst-rich, devitrified ignimbrite. Both phenocrysts and pumice range from 8 to 15 vol %. Lithic clasts are rare throughout the ash flow, typically representing less than 1 vol %. Color ranges from grayish pink (5R 8/2) to pale red (5R 6/2) to moderate pink (5R 7/4).

The unit is nonwelded at the top, progresses in degree of welding to a moderately welded interval (typically near 30-ft depth), and then becomes nonwelded tuff near the bottom. One core hole (SHB-CMR-1) has a small, densely welded zone at a depth of approximately 20 to 21 ft.

Phenocrysts in Unit 4 are dominated by quartz and sanidine, with minor plagioclase and altered mafic minerals. Whole quartz crystals are approximately 2 mm on edge, and make up 5 to 7 vol % of the tuff. Feldspars are similar to quartz in size (2 to 3 mm) and abundance (approximately 5 vol %). The quartz and feldspar phenocrysts of this unit have the same distinctive physical characteristics described for Unit 3 (bipyramidal quartz, blue chatoyant sanidine). The rare and small (<1 mm) mafic phenocrysts make up only 1 to 2 vol %.

Pumices in Unit 4 range in size from 5 mm to over 6 cm and display a variety of colors. All the pumices are devitrified. Pumices in the upper portion of Unit 4 (beginning at 15 to 17 ft depth) are vapor-phase altered, often deep brown or purple in color with gray cores, and are characterized by minute acicular crystals growing within the tubes of the pumice. Binocular microscopy indicates that the primary vapor phase alteration minerals are cristobalite and sanidine. Pumices in the nonwelded to slightly welded portions of this unit are fully inflated and show little or no deformation, but the primary pumice textures are often obliterated by devitrification processes. In the central portion of the unit (approximately 25 to 35 ft depth), where welding is moderate, the pumices are significantly elongated and aligned parallel to bedding. Their color is either dark gray or orange pink, similar to the ash matrix. There is a rhythmic banding in the lower portion of the unit (from a depth of 35 ft to the base of the unit) whose cause is unknown. The bands consist of a moderate brown-colored alteration of the tuff on a 1 to 2 cm scale alternating with the more typical orange-pink matrix.

Lithic fragments in Unit 4 are rare, typically less than 1 vol % of the tuff and less than 8-mm in diameter. The lithic fragments are often altered to a powdery lime-green material surrounded by an intense white alteration rim extending several millimeters into the enclosing tuff matrix. Despite a low volume percentage, the lithic fragments are present throughout Unit 4.

The matrix of Unit 4 is composed of ash shards, small pumice fragments, and minute phenocryst fragments. The prevalent colors of the matrix in Unit 4 are pinkish gray to orange pink to pale red. The induration of the cores does not closely match the degree of welding. Some intervals displayed moderately to densely welded core that was relatively friable and, in some instances, nonindurated. However, much of the moderately to densely welded core samples were recovered as 2 to 5 cm-thick disks of indurated core surrounded by rock powder in the core barrel, an effect resulting from drilling action.

A thin, crystal-rich, medium-to-coarse grained, unconsolidated sandy surge is present at the base of Unit 4 in all nine core holes. In addition to the basal surge deposit, core holes SHB-CMR-2 and SHB-CMR-3 contain 1 to 2 additional surges within the lower portion of Unit 4. Surge thicknesses vary from 0.2 feet (SHB-CMR-1, SHB-CMR-4) to 2.2 feet (SHB-CMR-8). The surge intervals contain 60% to 90% crystals of quartz and sanidine with the remainder of the material being fine ash. The samples of surge recovered in the core are massive-to-laminar bedded.

Post-Bandelier Tuff Sediments Lithologic Description

Overlying Unit 4 of the Bandelier Tuff is a thin layer of dark-colored alluvium and weathered tuff fragments ranging in thickness from 0 ft to about 20 ft, averaging <1 ft thick in the core holes. The alluvium forms a wedge that pinches out to the west. In several cores, particularly in SHB-CMR-10, the "alluvium" consists of disturbed alluvium, construction fill, and tuff rubble, probably associated with the original construction of the CMR building in 1952. In some core holes, thin, subhorizontal (<1-inch) clay seams can be found within sand- and gravel-sized material. Where the alluvium is thickest, it typically contains rubblized, weathered pieces of Unit 4 tuff, and it is not always possible to pinpoint the first appearance in the core of *in situ* Unit 4. Note that this fact has no bearing on the present geological interpretation for the area because deeper contacts associated with Units 3t and 3 were used for geologic structure analysis. The limited thickness, lack of marker beds, and extensive disturbance of the post-Bandelier alluvium make other near-surface geologic investigations of faulting (e.g., trenching) impractical at the site.

V. GEOCHEMISTRY

Geochemical results from XRF analysis of core samples yield characteristic signatures for different units of the Tshirege Member (Broxton and Gardner, personal communication; Warren et al., 1998). Systematic variations in the amount of silica (SiO₂), titanium (TiO₂), and zirconium (Zr) correlate with changes in lithologic character of the tuffs and can be used to differentiate and pinpoint contacts between different flow units (Stimac et al., in preparation). Krier et al. (1998) used this information to locate contacts between marker beds to within about 1 ft in drill cores taken for geological analysis at proposed LANL building sites. This same analysis approach is used in the present study at the CMR site.

Table 3 lists the results of XRF analyses for samples from the SHB-CMR cores. Only elements and compounds with results above their respective detection levels are listed. Empirically, Unit 3 titanium contents are considered to be less than 0.15 wt% TiO₂, Unit 3t titanium contents fall between 0.15 wt% and 0.18 wt% TiO₂, and Unit 4 titanium contents are >0.20 wt% TiO₂. Similar divisions are assigned to Zr contents; generally, Unit 3t has Zr content between about 250 ppm and 350 ppm. The Zr discriminator is not compatible everywhere because holes SHB-CMR-5, SHB-CMR-6, and SHB-CMR-8 have Unit 4 samples with Zr contents of 336 ppm, 332 ppm, and 336 ppm, respectively. Nonetheless, there is

consistency in the ranges of these signature analytes throughout the sequence of rocks within this part of the Tshirege Member. Silica (SiO_2) does not display as regular a distribution as the other analytes, but clearly increases in abundance down-section from Unit 4 to Unit 3. Our analyses average about 74.7 wt% SiO_2 in Unit 4, 75.7 wt% SiO_2 in Unit 3t, and 77.9 wt% SiO_2 in Unit 3.

Figures 4 through 12 compare XRF results for these three analytes, lithologic mapping (reflected as welding character and surge intervals), and stratigraphic assignments for each of the nine core holes for the depths of interest. There is a strong correlation between distinct chemical variations and the occurrence of surge deposits, which often physically define the boundaries between the three different units. In each core, surge deposits at the base of Unit 4 and Unit 3t consistently mark stratigraphic contacts as determined by distinct changes in lithologies in the cores and steep chemical trends in SiO_2 , TiO_2 , and Zr. Two minor exceptions are: (1) SHB-CMR-4, which, lacking a surge deposit at the Unit 3t base, nonetheless exhibits the characteristic increase in SiO_2 and decreases in TiO_2 and Zr at the Unit 3t/3 boundary, and (2) SHB-CMR-2, which has a surge deposit at the top of Unit 3 in addition to the overlying surge at the base of Unit 3t. The consistency of the chemical variations and their relation to lithologic changes in the cores yield high accuracy in assigning elevations to significant contacts.

In SHB-CMR-10, five surge deposits were described in the interval from 42 ft to 60 ft. The upper two surges define the bases of Unit 4 and Unit 3t, but the lower three surges occur within and toward the top of Unit 3 tuff. The sample at 54.0 ft, located immediately above the deep surge in Unit 3, exhibits SiO_2 (76.6 wt%) and Zr (243 ppm) contents somewhat ambiguous with respect to Unit 3 assignment. The sample's TiO_2 content (0.135 wt%) is the criterion employed here to assign this sample to Unit 3 and maintain the Unit 3t/3 contact relatively higher in the core hole. Although Unit 4 tuff is known to contain additional thin surge deposits above its basal contact in outcrops near TA-3, none were observed in these cores.

Analytical results from core hole SHB-CMR-6 show the expected trends in SiO_2 , TiO_2 , and Zr through the intervals of interest, but exhibit a reversal in chemical trends toward the bottom of the hole (Figure 9). The compositions of these deeper samples resemble the signatures of overlying rocks in several details. In previous drilling at TA-3, a plot of Ba and TiO_2 was shown to strongly differentiate among Units 3, 3t, and 4 (Krier et al., 1998). Figure 13 shows the same differentiation using results for Ba and Zr analyses for SHB-CMR-6. Although Ba shows less consistent variation with stratigraphic position than Zr in both this and the previous study (partly because of the relatively large uncertainties in analysis by XRF), the plot indicates that Unit 3t chemistry may be present in the interval from 47.5 to 50.7 ft as well as below 55.0 ft. Indeed, detailed mapping of the core shows repeated sections of distinct lithologic character in the intervals from 52.5 to 53.2 ft and 55.0 to 57.5 ft (the total depth of hole), that is, evidence of a repeated intervals of Unit 3 and Unit 3t. As discussed in the next section, these data indicate that two reverse faults cut the SHB-CMR-6 core hole.

VI. GEOLOGIC STRUCTURE

We have analyzed the three-dimensional positions of correlated stratigraphic markers among the core holes to evaluate the possibility of vertical offsets caused by faulting beneath the CMR building. A computer-generated, three-dimensional surface model of the top of Unit 3 and intercore hole cross sections define our interpretation of all data presented.

Table 3. X-ray fluorescence analyses for SHB-CMR core samples.

Sample Number	Hole Elev. (ft)	Depth (ft)	Sample Elev. (ft)	Unit	SiO ₂ wt%	TiO ₂ wt%	Al ₂ O ₃ wt%	Fe ₂ O ₃ wt%	MnO wt%	MgO wt%	CaO wt%	Na ₂ O wt%	K ₂ O wt%	P ₂ O ₅ wt%	LOI %
SHB-CMR-1/46.0	7402.2	46.0	7356.2	4	75.28	0.231	13.16	2.12	0.07	0.17	0.54	4.41	4.72	0.03	0.21
SHB-CMR-1/47.0	7402.2	47.0	7355.2	3t	75.84	0.179	12.87	1.89	0.06	-0.11	0.33	4.41	4.84	0.02	0.25
SHB-CMR-1/49.0	7402.2	49.0	7353.2	3t	75.81	0.178	12.82	1.90	0.07	-0.11	0.30	4.41	4.93	0.02	0.18
SHB-CMR-1/59.0	7402.2	59.0	7343.2	3	76.79	0.127	12.48	1.74	0.05	0.12	0.31	3.94	4.34	0.01	0.74
SHB-CMR-1/62.0	7402.2	62.0	7340.2	3	77.08	0.135	12.29	1.67	0.05	-0.11	0.31	4.00	4.29	0.01	0.55
SHB-CMR-2/41.5	7399.8	41.5	7358.3	4	75.25	0.211	12.77	2.14	0.08	0.20	0.48	4.15	4.41	0.03	0.56
SHB-CMR-2/48.5	7399.8	48.5	7351.3	3t	75.95	0.177	12.77	1.82	0.07	-0.11	0.29	4.41	4.83	0.02	0.20
SHB-CMR-2/49.9	7399.8	49.9	7349.9	3t	76.40	0.166	12.76	1.79	0.06	-0.11	0.29	4.42	4.77	0.02	0.23
SHB-CMR-2/51.0	7399.8	51.0	7348.8	3	78.80	0.136	11.25	1.54	0.06	-0.11	0.38	3.86	3.97	0.01	0.18
SHB-CMR-2/54.1	7399.8	54.1	7345.7	3	78.96	0.123	11.76	1.47	0.05	-0.11	0.29	4.08	4.38	0.01	0.15
SHB-CMR-2/55.8	7399.8	55.8	7344.0	3	78.27	0.122	11.82	1.47	0.05	-0.11	0.28	4.01	4.37	0.01	0.22
SHB-CMR-2/58.8	7399.8	58.8	7341.0	3	77.22	0.151	12.33	1.81	0.07	-0.11	0.32	4.11	4.39	0.01	0.41
SHB-CMR-2/61.8	7399.8	61.8	7338.0	3	77.42	0.128	12.29	1.60	0.06	-0.11	0.29	4.10	4.47	0.01	0.35
SHB-CMR-3/35.8	7398.6	35.8	7362.8	4	74.64	0.238	13.16	2.23	0.08	0.19	0.53	4.43	4.71	0.04	0.32
SHB-CMR-3/38.8	7398.6	38.8	7359.8	4	74.94	0.291	12.71	2.74	0.10	0.20	0.62	4.33	4.41	0.04	0.30
SHB-CMR-3/40.2	7398.6	40.2	7358.4	3t	75.95	0.188	12.90	1.93	0.08	-0.11	0.30	4.37	4.83	0.02	0.29
SHB-CMR-3/44.8	7398.6	44.8	7353.8	3t	75.63	0.193	13.16	2.03	0.08	0.12	0.41	4.18	4.65	0.02	0.70
SHB-CMR-3/45.1	7398.6	45.1	7353.5	3t	76.40	0.173	12.82	1.83	0.08	-0.11	0.36	4.33	4.75	0.02	0.25
SHB-CMR-3/46.0	7398.6	46.0	7352.6	3	79.76	0.141	10.76	1.64	0.08	-0.11	0.43	3.78	3.92	0.01	0.14
SHB-CMR-3/49.6	7398.6	49.6	7349.0	3	77.93	0.126	11.78	1.56	0.06	-0.11	0.33	4.09	4.37	0.01	0.17
SHB-CMR-3/51.5	7398.6	51.5	7347.1	3	78.16	0.126	12.00	1.57	0.06	-0.11	0.32	4.16	4.43	0.01	0.19
SHB-CMR-4/29.5	7398.4	29.5	7368.9	4	74.80	0.252	13.15	2.28	0.08	0.18	0.61	4.52	4.68	0.04	0.29
SHB-CMR-4/31.7	7398.4	31.7	7366.7	4	74.41	0.231	13.20	2.17	0.07	0.18	0.57	4.40	4.67	0.03	0.30
SHB-CMR-4/34.6	7398.4	34.6	7363.8	4	73.93	0.226	13.51	2.32	0.07	0.21	0.53	4.35	4.64	0.03	0.76
SHB-CMR-4/38.7	7398.4	38.7	7359.7	3t	75.86	0.176	12.79	1.89	0.06	-0.11	0.28	4.34	4.81	0.02	0.24
SHB-CMR-4/41.7	7398.4	41.7	7356.7	3t	76.31	0.170	12.75	1.83	0.07	-0.11	0.27	4.40	4.75	0.02	0.21
SHB-CMR-4/43.8	7398.4	43.8	7354.6	3	76.84	0.131	12.52	1.69	0.05	-0.11	0.31	3.99	4.40	0.01	0.63
SHB-CMR-4/46.7	7398.4	46.7	7351.7	3	78.05	0.123	12.26	1.54	0.05	-0.11	0.28	4.04	4.42	0.01	0.21
SHB-CMR-4/48.5	7398.4	48.5	7349.9	3	77.92	0.124	12.14	1.61	0.05	-0.11	0.29	4.03	4.35	0.01	0.29
SHB-CMR-4/50.1	7398.4	50.1	7348.3	3	77.92	0.127	12.10	1.65	0.05	-0.11	0.28	4.05	4.46	-0.01	0.14
SHB-CMR-5/31.1	7397.5	31.1	7366.4	4	73.98	0.238	13.49	2.37	0.08	0.23	0.49	4.34	4.61	0.03	0.91
SHB-CMR-5/34.0	7397.5	34.0	7363.5	3t	74.10	0.167	12.80	1.93	0.07	-0.11	0.30	4.40	4.80	0.02	0.44

Table 3. (continued)

Sample Number	Hole Elev. (ft)	Depth (ft)	Sample Elev. (ft)	Unit	SiO ₂ wt%	TiO ₂ wt%	Al ₂ O ₃ wt%	Fe ₂ O ₃ wt%	MnO wt%	MgO wt%	CaO wt%	Na ₂ O wt%	K ₂ O wt%	P ₂ O ₅ wt%	LOI wt%
SHB-CMR-5/35.1	7397.5	35.1	7362.4	3t	75.93	0.176	13.04	1.98	0.07	-0.11	0.31	4.43	4.76	0.02	0.33
SHB-CMR-5/37.1	7397.5	37.1	7360.4	3t	76.39	0.176	12.73	1.86	0.07	-0.11	0.29	4.43	4.79	0.01	0.17
SHB-CMR-5/38.6	7397.5	38.6	7358.9	3t	75.44	0.176	13.02	2.08	0.07	0.16	0.35	4.22	4.59	0.02	0.71
SHB-CMR-5/39.6	7397.5	39.6	7357.9	3	77.81	0.123	12.09	1.56	0.06	-0.11	0.29	4.18	4.46	-0.01	0.18
SHB-CMR-5/40.8	7397.5	40.8	7356.7	3	78.06	0.122	12.01	1.52	0.06	-0.11	0.28	4.16	4.41	-0.01	0.16
SHB-CMR-6/46.5	7392.2	46.5	7345.7	4	75.21	0.23	12.93	2.12	0.07	0.15	0.47	4.45	4.72	0.04	0.19
SHB-CMR-6/48.0	7392.2	48.0	7344.2	3t	76.05	0.17	12.80	1.79	0.08	-0.11	0.34	4.47	4.80	0.02	0.25
SHB-CMR-6/49.0	7392.2	49.0	7343.2	3t	76.17	0.18	12.82	1.85	0.08	-0.11	0.29	4.46	4.81	0.01	0.17
SHB-CMR-6/50.2	7392.2	50.2	7342.0	3	77.62	0.13	11.99	1.62	0.06	-0.11	0.31	4.12	4.42	0.01	0.16
SHB-CMR-6/51.1	7392.2	51.1	7341.1	3	77.86	0.13	12.06	1.58	0.06	-0.11	0.33	4.19	4.41	0.01	0.16
SHB-CMR-6/52.1	7392.2	52.1	7340.1	3	77.90	0.12	12.09	1.52	0.05	-0.11	0.28	4.22	4.51	0.01	0.13
SHB-CMR-6/52.6	7392.2	52.6	7339.6	3	78.84	0.14	11.30	1.67	0.06	-0.11	0.42	3.90	4.11	0.01	0.12
SHB-CMR-6/54.1	7392.2	54.1	7338.1	3	77.54	0.13	12.04	1.63	0.06	-0.11	0.31	4.22	4.47	0.01	0.11
SHB-CMR-6/55.0	7392.2	55.0	7337.2	3t	75.76	0.18	12.65	1.86	0.09	-0.11	0.27	4.45	4.88	0.01	0.23
SHB-CMR-6/56.1	7392.2	56.1	7336.1	3t	75.73	0.18	12.73	1.87	0.08	-0.11	0.28	4.43	4.89	0.02	0.16
SHB-CMR-6/57.5	7392.2	57.5	7334.7	3t	75.91	0.17	12.73	1.84	0.08	-0.11	0.27	4.47	4.78	0.02	0.20
SHB-CMR-7/44.0	7394.9	44.0	7350.9	4	74.78	0.230	13.19	2.17	0.07	0.16	0.50	4.49	4.75	0.04	0.14
SHB-CMR-7/48.0	7394.9	48.0	7346.9	3t	76.65	0.179	12.54	1.87	0.07	-0.11	0.31	4.30	4.77	0.02	0.15
SHB-CMR-7/50.5	7394.9	50.5	7344.4	3t	75.69	0.174	12.75	1.86	0.07	-0.11	0.35	4.42	4.83	0.02	0.17
SHB-CMR-7/54.1	7394.9	54.1	7340.8	3	77.87	0.129	11.98	1.58	0.06	-0.11	0.36	4.08	4.41	0.01	0.05
SHB-CMR-8/35.5	7392.7	35.5	7357.2	4	74.21	0.241	13.17	2.31	0.06	0.16	0.50	4.44	4.68	0.03	0.25
SHB-CMR-8/40.0	7392.7	40.0	7352.7	4	74.57	0.225	13.36	2.25	0.06	0.13	0.45	4.45	4.74	0.03	0.23
SHB-CMR-8/44.0	7392.7	44.0	7348.7	3t	73.82	0.181	13.72	2.28	0.06	0.22	0.35	4.17	4.58	0.02	1.44
SHB-CMR-8/46.5	7392.7	46.5	7346.2	3	77.81	0.122	11.80	1.48	0.05	-0.11	0.27	4.17	4.45	-0.01	0.12
SHB-CMR-8/49.0	7392.7	49.0	7343.7	3	77.52	0.124	11.94	1.53	0.06	-0.11	0.29	4.25	4.54	0.01	0.11
SHB-CMR-10/41.0	7398.4	41.0	7357.4	4	74.70	0.234	13.18	2.22	0.11	0.19	0.48	4.41	4.74	0.03	0.33
SHB-CMR-10/43.1	7398.4	43.1	7355.3	3t	75.54	0.177	12.69	1.84	0.06	-0.11	0.30	4.46	4.78	0.02	0.17
SHB-CMR-10/46.6	7398.4	46.6	7351.8	3t	76.16	0.176	12.56	1.89	0.07	-0.11	0.27	4.46	4.82	0.02	0.14
SHB-CMR-10/48.0	7398.4	48.0	7350.4	3t	74.60	0.158	12.38	1.73	0.06	-0.11	0.28	4.48	4.81	0.01	0.15
SHB-CMR-10/51.5	7398.4	51.5	7346.9	3	77.64	0.144	11.69	1.65	0.07	-0.11	0.40	4.16	4.38	0.01	0.02
SHB-CMR-10/54.0	7398.4	54.0	7344.4	3	76.63	0.135	11.83	1.61	0.06	-0.11	0.39	4.13	4.45	0.01	0.09
SHB-CMR-10/56.5	7398.4	56.5	7341.9	3	79.24	0.117	11.23	1.38	0.05	-0.11	0.35	3.94	4.19	0.01	0.09

Table 3. (continued)

Sample Number	Unit	Total Major wt%	V ppm	Cr ppm	Ni ppm	Zn ppm	Rb ppm	Sr ppm	Y ppm	Zr ppm	Nb ppm	Ba ppm	Total Trace wt%	Total + LOI wt%
SHB-CMR-1/46.0	4	100.74	-9.89	-7.91	-10.05	65.58	87.05	56.96	34.89	341.67	43.48	321.14	0.12	101.07
SHB-CMR-1/47.0	3t	100.44	-9.76	-7.85	-10.68	59.46	94.68	26.57	36.60	330.59	52.87	181.72	0.10	100.79
SHB-CMR-1/49.0	3t	100.43	-9.74	-7.89	-10.67	65.12	103.14	24.22	41.19	320.56	53.33	172.10	0.10	100.70
SHB-CMR-1/59.0	3	99.91	-9.68	-7.92	-10.06	48.80	97.66	33.99	37.05	220.52	45.74	177.37	0.08	100.73
SHB-CMR-1/62.0	3	99.85	-9.71	11.98	-10.06	61.36	92.76	35.49	35.32	216.30	41.66	201.40	0.09	100.49
SHB-CMR-2/41.5	4	99.72	-9.85	-7.93	-10.06	68.23	95.30	60.88	37.20	292.49	41.93	277.01	0.11	100.38
SHB-CMR-2/48.5	3t	100.33	-9.76	-7.95	-10.06	69.03	96.92	23.63	32.38	319.76	51.43	225.34	0.10	100.63
SHB-CMR-2/49.9	3t	100.67	-9.73	-7.88	-10.05	75.18	97.71	28.18	33.07	311.97	48.14	123.85	0.09	101.00
SHB-CMR-2/51.0	3	100.00	-9.70	-7.94	-10.07	45.55	73.48	46.00	27.04	172.92	28.41	201.70	0.07	100.26
SHB-CMR-2/54.1	3	101.13	-9.65	-7.93	-10.07	55.67	98.06	37.24	22.25	219.77	48.53	168.23	0.08	101.35
SHB-CMR-2/55.8	3	100.40	-9.68	-7.93	-10.06	41.52	94.89	30.38	37.56	237.56	53.59	129.59	0.08	100.70
SHB-CMR-2/58.8	3	100.42	-9.72	-7.96	-10.07	69.29	108.83	45.39	40.31	242.42	58.08	157.53	0.09	100.91
SHB-CMR-2/61.8	3	100.36	12.74	-7.94	-10.71	68.45	99.78	32.95	37.43	233.11	41.88	167.97	0.09	100.80
SHB-CMR-3/35.8	4	100.25	-9.90	-7.94	-10.06	81.52	91.97	51.58	33.52	352.65	49.77	277.12	0.12	100.69
SHB-CMR-3/38.8	4	100.38	-10.08	-7.95	-10.05	89.23	65.55	64.66	25.83	342.46	44.69	309.50	0.12	100.80
SHB-CMR-3/40.2	3t	100.57	-9.78	-7.91	-10.06	66.57	102.57	28.16	44.05	333.78	55.78	181.38	0.10	100.96
SHB-CMR-3/44.8	3t	100.47	-9.80	-7.94	-10.06	63.58	103.69	30.31	37.38	336.74	57.49	185.70	0.10	101.28
SHB-CMR-3/45.1	3t	100.76	-9.73	-7.92	-10.06	70.76	107.64	24.97	32.13	319.17	61.74	186.56	0.10	101.11
SHB-CMR-3/46.0	3	100.53	-9.69	-7.92	-10.06	42.92	78.62	36.82	30.20	213.43	36.80	158.05	0.07	100.74
SHB-CMR-3/49.6	3	100.26	-9.65	-7.88	-10.05	56.62	96.03	32.50	31.60	235.01	44.61	143.95	0.08	100.51
SHB-CMR-3/51.5	3	100.84	-9.64	-7.91	-10.05	51.64	104.14	29.88	42.52	243.10	53.12	134.19	0.08	101.11
SHB-CMR-4/29.5	4	100.59	-9.94	-7.91	-10.05	65.85	86.44	58.85	30.54	372.77	40.30	296.33	0.12	101.00
SHB-CMR-4/31.7	4	99.94	15.72	-7.91	-10.67	65.20	83.42	68.54	36.51	338.20	54.10	296.84	0.12	100.36
SHB-CMR-4/34.6	4	99.81	-9.85	-7.91	-10.05	61.63	88.11	58.49	37.67	331.55	40.67	291.36	0.11	100.69
SHB-CMR-4/38.7	3t	100.23	-9.73	-7.89	-10.05	67.16	99.34	26.57	32.21	342.14	52.95	215.51	0.10	100.58
SHB-CMR-4/41.7	3t	100.57	11.60	-7.89	-10.06	69.03	93.80	29.70	39.45	326.15	46.89	201.19	0.10	100.88
SHB-CMR-4/43.8	3	99.95	-9.67	-7.96	-10.72	71.37	98.95	34.87	40.53	240.63	56.15	138.76	0.09	100.66
SHB-CMR-4/46.7	3	100.78	-9.62	-7.91	-10.06	59.40	112.51	32.23	40.70	234.98	41.31	168.02	0.09	101.08
SHB-CMR-4/48.5	3	100.54	-9.64	-7.92	-10.06	60.40	102.94	33.39	33.29	231.49	46.65	158.34	0.08	100.91
SHB-CMR-4/50.1	3	100.64	-9.65	123.12	22.91	73.40	106.19	34.87	46.94	235.30	55.17	158.39	0.11	100.89
SHB-CMR-5/31.1	4	99.84	-11.25	-7.91	-10.05	73.16	97.22	53.25	33.75	335.96	47.66	256.83	0.11	100.87
SHB-CMR-5/34.0	3t	98.58	-9.74	-7.95	-10.07	69.99	103.15	29.30	38.97	308.69	41.78	147.86	0.09	99.11

Table 3. (continued)

Sample Number	Unit	Total Major wt%	V ppm	Cr ppm	Ni ppm	Zn ppm	Rb ppm	Sr ppm	Y ppm	Zr ppm	Nb ppm	Ba ppm	Total Trace wt%	Total + LOI wt%
SHB-CMR-5/35.1	3t	100.70	-9.72	-7.90	-10.06	73.43	103.36	28.23	45.37	346.14	49.56	186.31	0.10	101.13
SHB-CMR-5/37.1	3t	100.74	-9.75	-7.93	-10.06	56.22	99.23	28.36	43.63	335.09	52.43	186.52	0.10	101.01
SHB-CMR-5/38.6	3t	100.13	-9.74	-7.92	-10.70	69.56	110.68	27.20	46.21	299.75	47.01	229.26	0.10	100.94
SHB-CMR-5/39.6	3	100.56	-9.65	-7.92	-10.06	50.44	109.26	29.04	30.58	242.68	52.00	168.08	0.08	100.83
SHB-CMR-5/40.8	3	100.62	-9.65	-7.91	-10.71	51.66	92.12	29.30	37.90	235.56	49.15	202.10	0.09	100.86
SHB-CMR-6/46.5	4	100.38	-9.84	10.79	-10.70	67.59	99.57	52.16	44.41	331.60	43.83	248.34	0.11	100.69
SHB-CMR-6/48.0	3t	100.52	-9.71	-7.87	-10.71	62.03	106.08	33.40	35.74	334.67	43.81	166.81	0.10	100.87
SHB-CMR-6/49.0	3t	100.67	-9.73	-7.90	-10.06	66.33	103.06	25.66	35.77	349.72	52.71	176.77	0.10	100.94
SHB-CMR-6/50.2	3	100.29	-9.60	93.52	40.17	35.93	100.06	35.21	37.90	248.34	45.38	143.61	0.10	100.55
SHB-CMR-6/51.1	3	100.63	-9.61	-7.89	-10.07	41.55	104.90	37.74	43.08	218.93	44.13	211.13	0.09	100.88
SHB-CMR-6/52.1	3	100.70	-9.67	-7.88	-10.06	45.41	105.21	28.55	40.03	230.16	60.06	115.13	0.08	100.90
SHB-CMR-6/52.6	3	100.46	-9.69	-7.95	-10.72	41.57	72.80	37.84	26.98	216.07	32.06	220.62	0.08	100.65
SHB-CMR-6/54.1	3	100.40	-9.68	-7.90	-10.07	45.10	109.34	34.21	43.11	234.13	40.87	192.18	0.09	100.59
SHB-CMR-6/55.0	3t	100.15	-9.71	-7.92	-10.71	50.26	103.82	29.02	31.35	314.41	51.84	186.13	0.10	100.48
SHB-CMR-6/56.1	3t	100.20	-9.77	-7.92	-10.06	57.67	112.11	24.99	37.58	337.48	47.27	162.30	0.10	100.46
SHB-CMR-6/57.5	3t	100.27	-9.74	-7.92	-11.02	43.54	109.23	25.99	38.51	333.93	60.72	176.44	0.10	100.57
SHB-CMR-7/44.0	4	100.39	-9.89	-7.91	-10.05	82.07	93.14	54.63	40.50	351.36	52.37	243.63	0.11	100.65
SHB-CMR-7/48.0	3t	100.71	-9.73	-7.88	-10.06	76.77	107.47	25.92	36.80	327.47	45.81	181.56	0.10	100.95
SHB-CMR-7/50.5	3t	100.17	-9.74	-7.94	-10.06	75.79	104.34	30.56	35.92	320.22	47.68	147.98	0.10	100.44
SHB-CMR-7/54.1	3	100.49	-9.69	-7.94	-10.06	55.81	104.19	32.71	39.51	247.58	37.95	134.28	0.08	100.62
SHB-CMR-8/35.5	4	99.80	-9.92	-7.93	-10.05	73.65	90.58	57.27	35.66	371.38	54.20	252.85	0.12	100.16
SHB-CMR-8/40.0	4	100.26	-9.88	-7.94	-10.05	74.86	92.96	58.80	37.24	336.20	45.14	267.72	0.11	100.61
SHB-CMR-8/44.0	3t	99.40	13.60	-7.96	-10.06	84.57	102.12	29.75	47.42	313.83	56.93	238.18	0.11	100.95
SHB-CMR-8/46.5	3	100.16	-9.65	-7.94	-10.07	54.73	100.20	23.57	41.92	250.45	60.28	144.13	0.08	100.36
SHB-CMR-8/49.0	3	100.26	-9.64	-7.93	-10.06	50.48	108.33	32.10	37.28	248.83	55.25	148.87	0.08	100.46
SHB-CMR-10/41.0	4	100.28	-9.90	-8.00	-10.06	62.37	94.05	53.35	45.28	359.76	52.20	267.45	0.12	100.74
SHB-CMR-10/43.1	3t	99.86	-9.76	-7.91	-10.06	64.64	101.51	23.38	39.07	329.17	55.50	162.29	0.10	100.13
SHB-CMR-10/46.6	3t	100.43	-9.77	-7.90	-10.06	68.91	94.33	29.13	37.51	328.38	63.62	147.94	0.10	100.67
SHB-CMR-10/48.0	3t	98.51	-9.71	-7.89	-10.06	64.82	106.56	28.29	46.55	302.20	54.61	211.25	0.10	98.75
SHB-CMR-10/51.5	3	100.14	-9.70	-7.90	-10.06	62.73	86.12	31.79	32.59	248.02	71.66	172.83	0.09	100.25
SHB-CMR-10/54.0	3	99.25	-9.71	-7.89	-10.07	59.88	102.50	42.16	30.68	243.04	49.81	187.47	0.09	99.43
SHB-CMR-10/56.5	3	100.50	-9.66	-7.90	-10.70	55.86	80.21	41.40	32.96	207.02	38.64	182.99	0.08	100.68

Concentrations preceded by a negative sign are below detection limits. Measurement uncertainties are available on request from the authors.

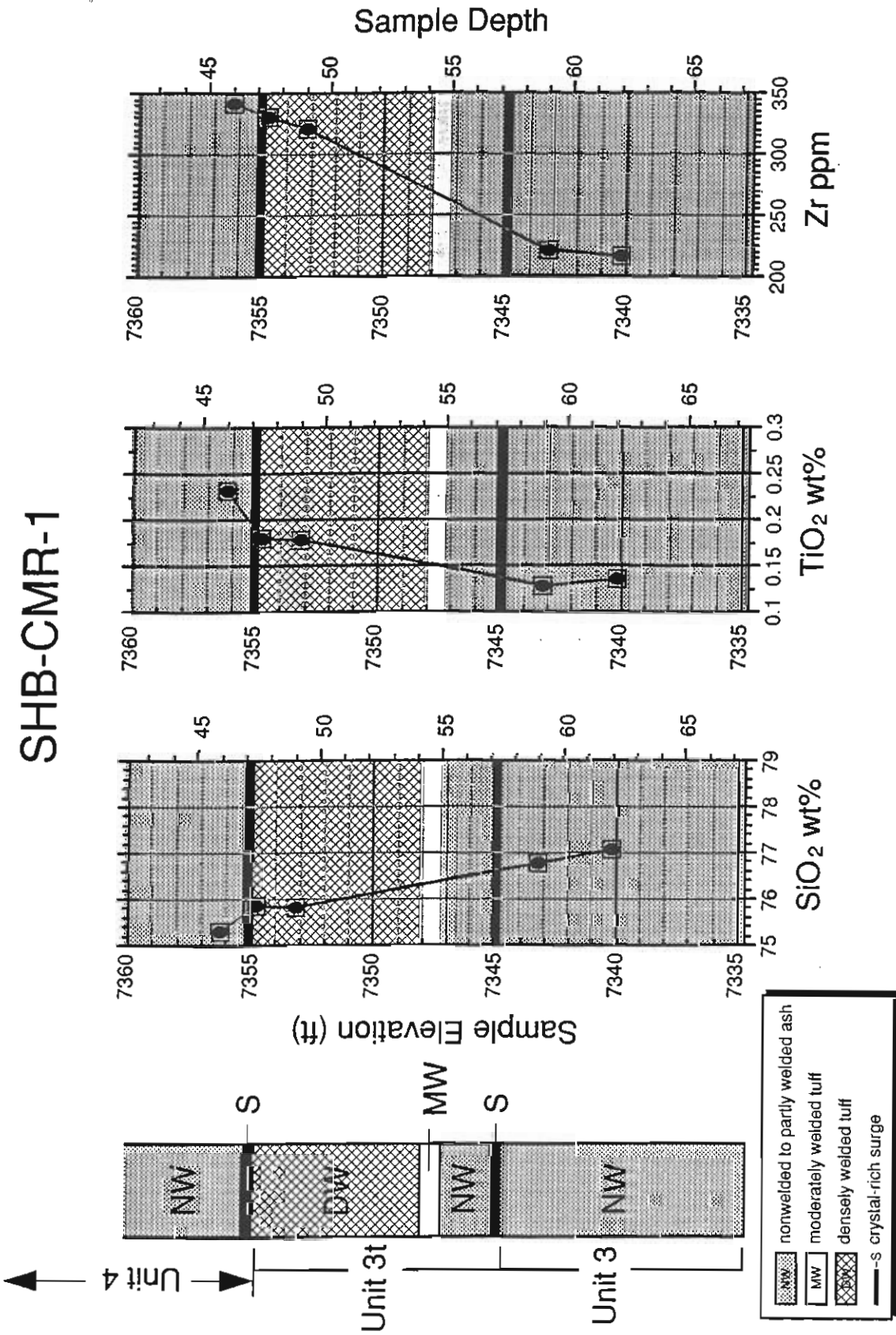


Figure 4. Stratigraphy, welding character, and surge locations compared with SiO₂, TiO₂, and Zr contents for core hole SHB-CMR-1.

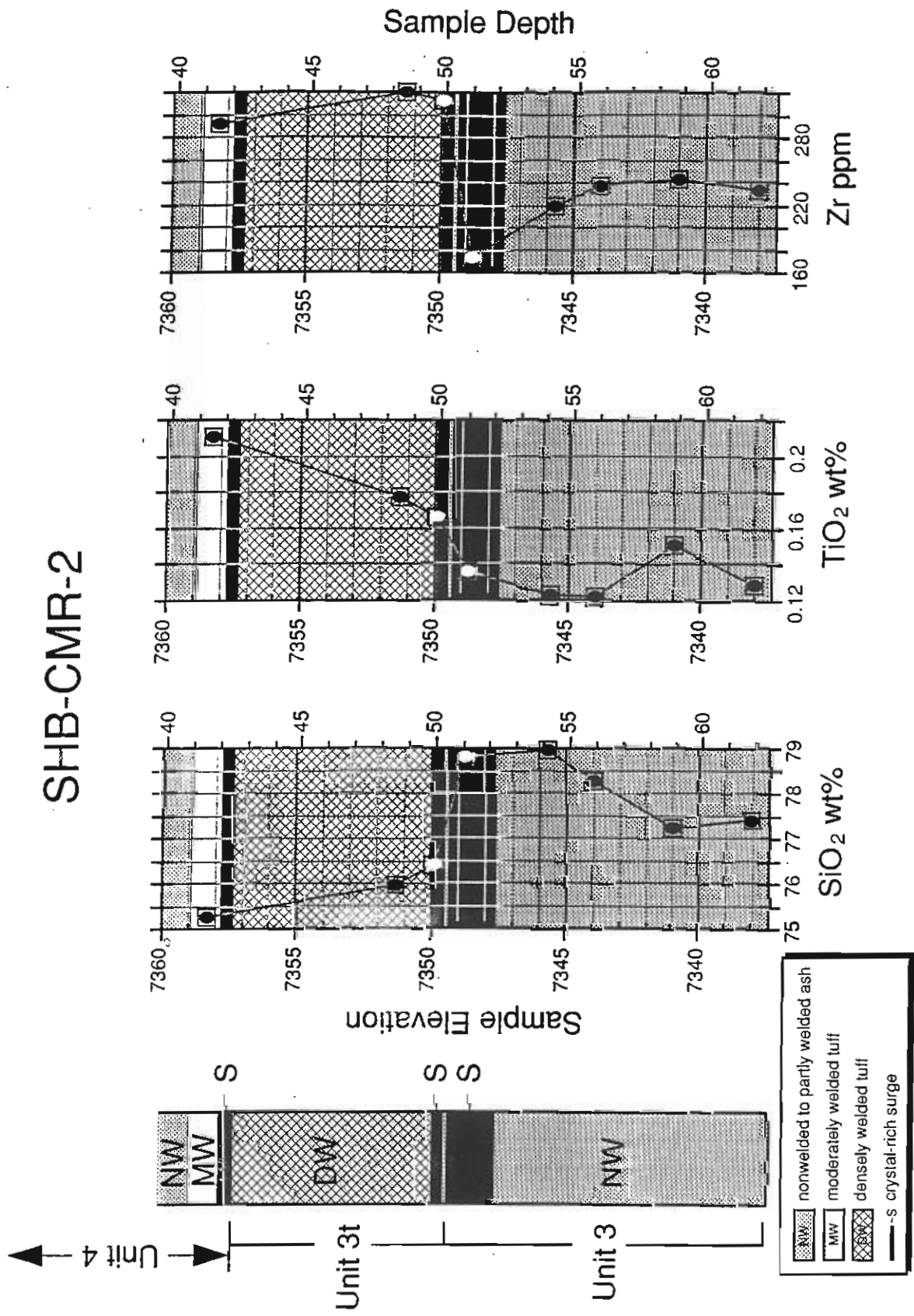


Figure 3 Stratigraphy, welding character, and surge locations compared with SiO₂, TiO₂, and Zr contents for core hole SHB-CMR-2.

SHB-CMR-3

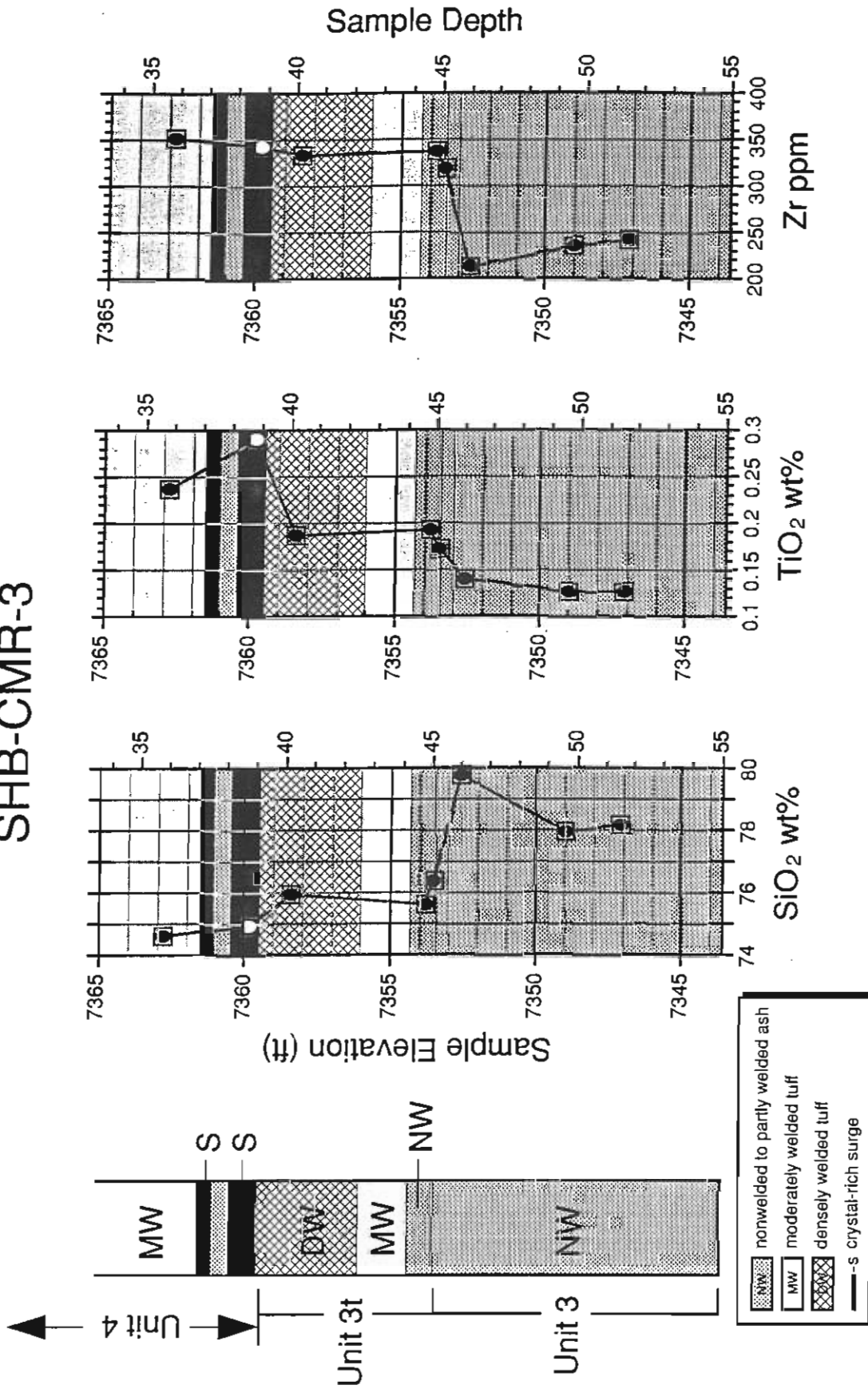


Figure 6. Stratigraphy, welding character, and surge locations compared with SiO₂, TiO₂, and Zr contents for core hole SHB-CMR-3.

SHB-CMR-4

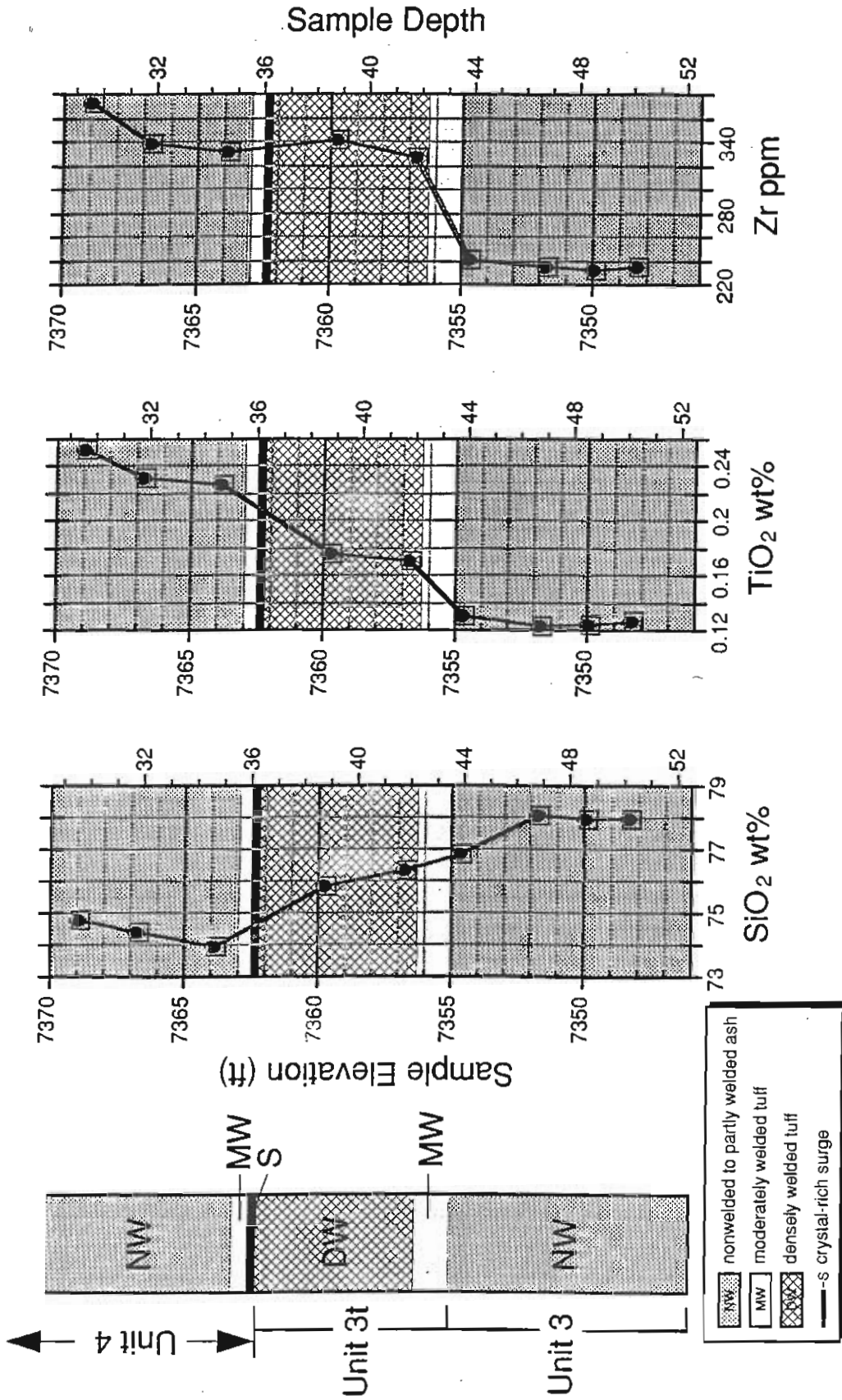


Figure 7. Stratigraphy, welding character, and surge locations compared with SiO₂, TiO₂, and Zr contents for core hole SHB-CMR-4.

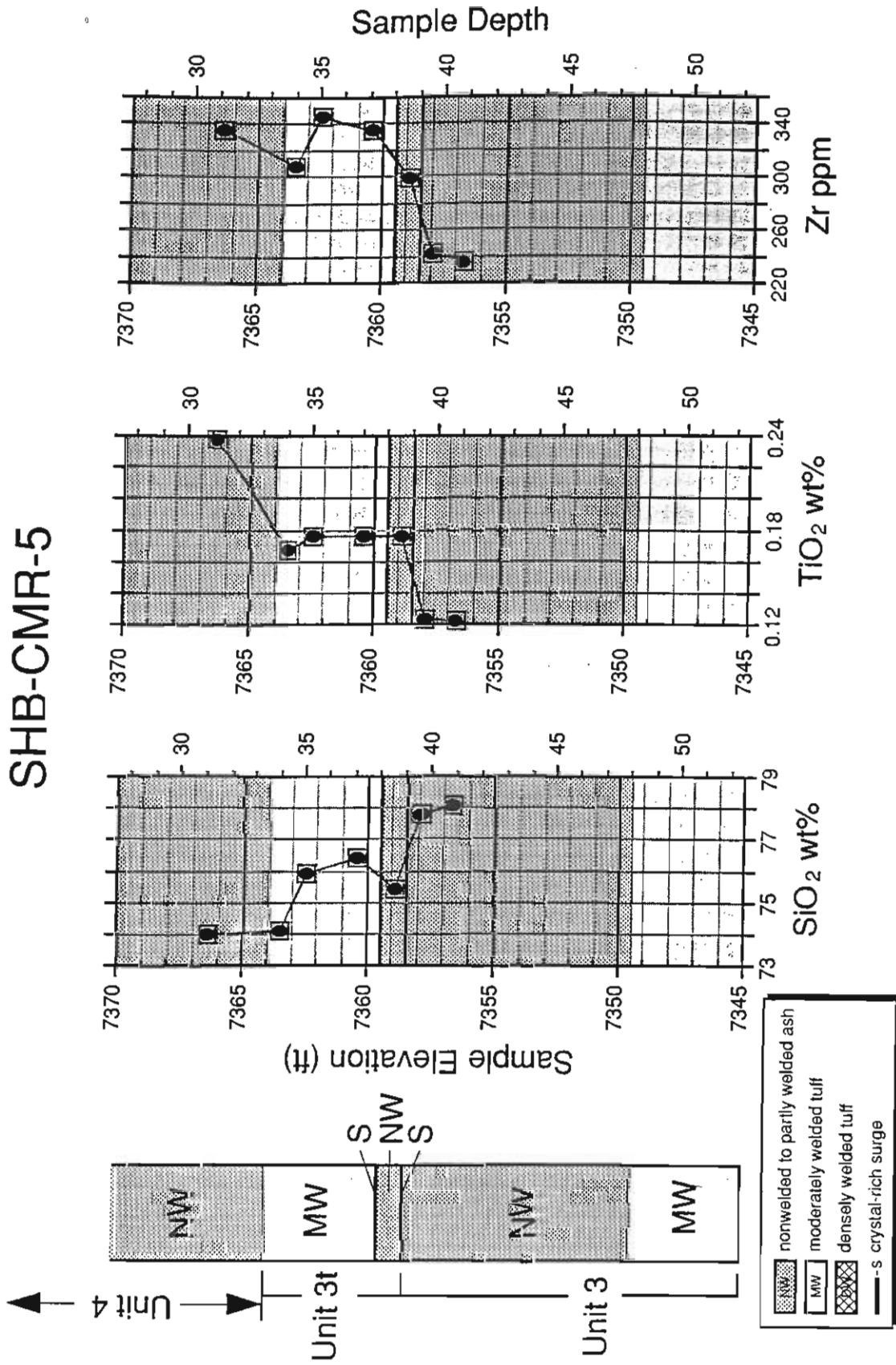


Figure 8. Stratigraphy, welding character, and surge locations compared with SiO₂, TiO₂, and Zr contents for core hole SHB-CMR-5.

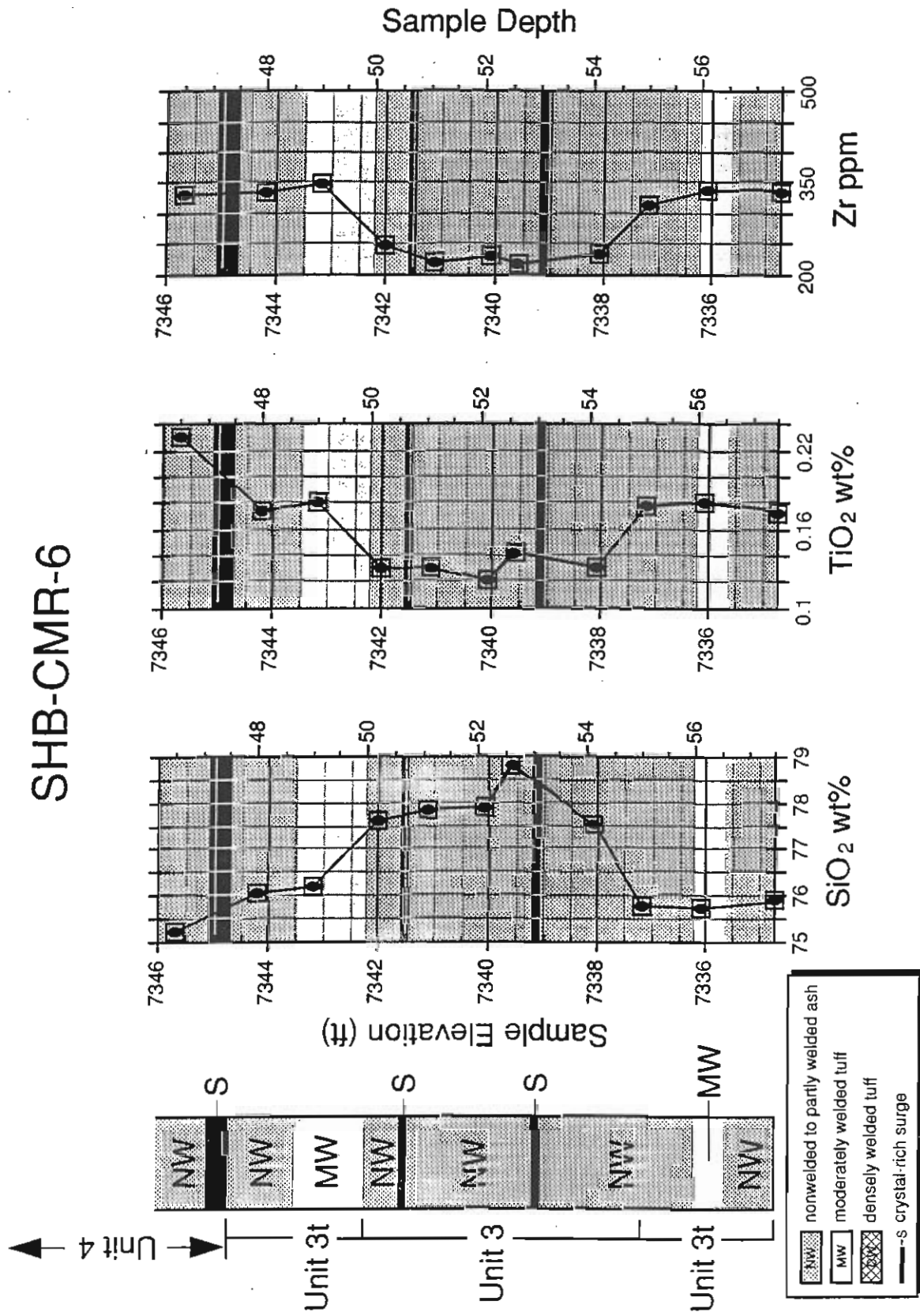


Figure 9. Stratigraphy, welding character, and surge locations compared with SiO₂, TiO₂, and Zr contents for core hole SHB-CMR-6.

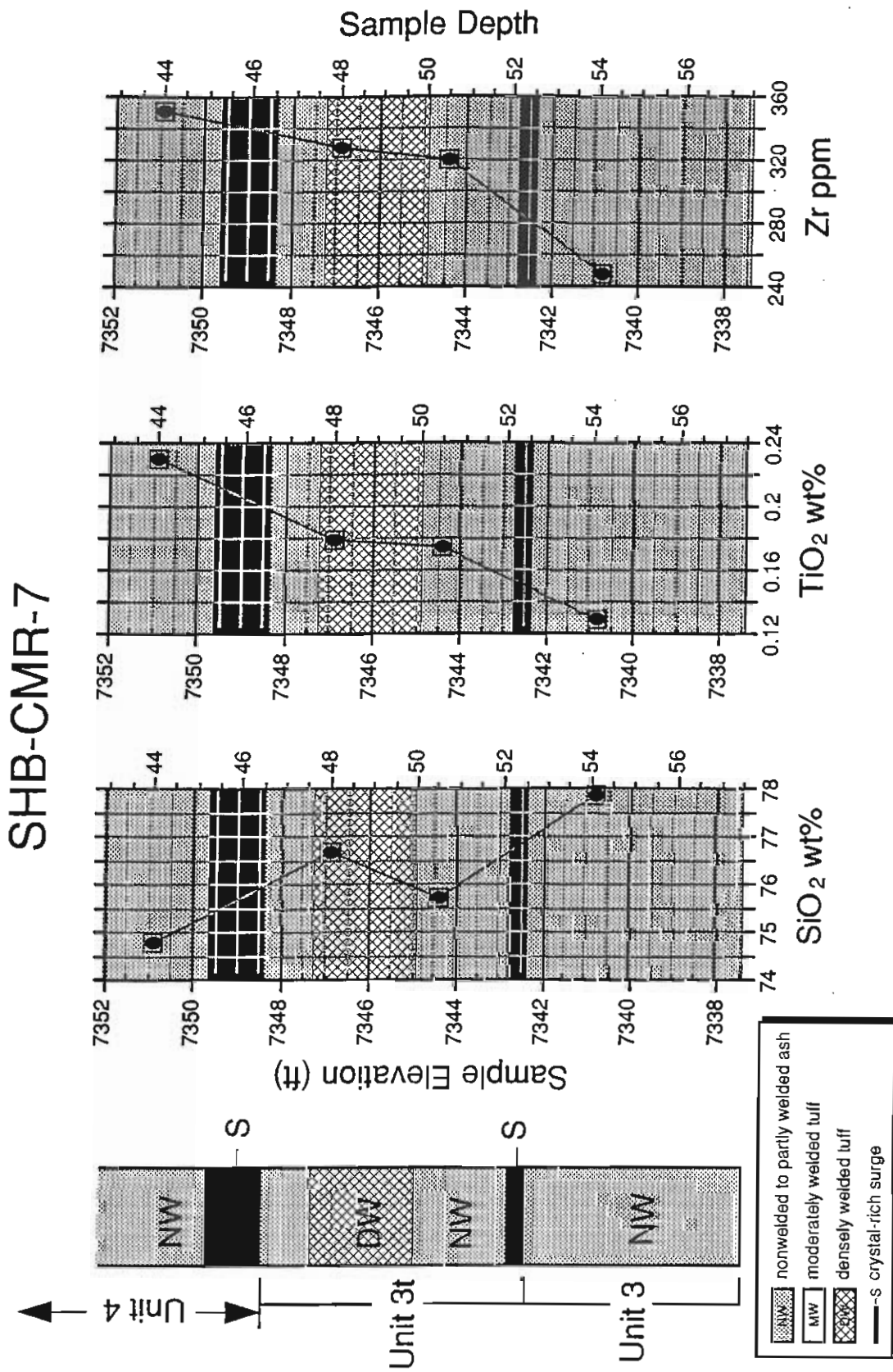


Figure 10. Stratigraphy, welding character, and surge locations compared with SiO₂, TiO₂, and Zr contents for core hole SHB-CMR-7.

SHB-CMR-8

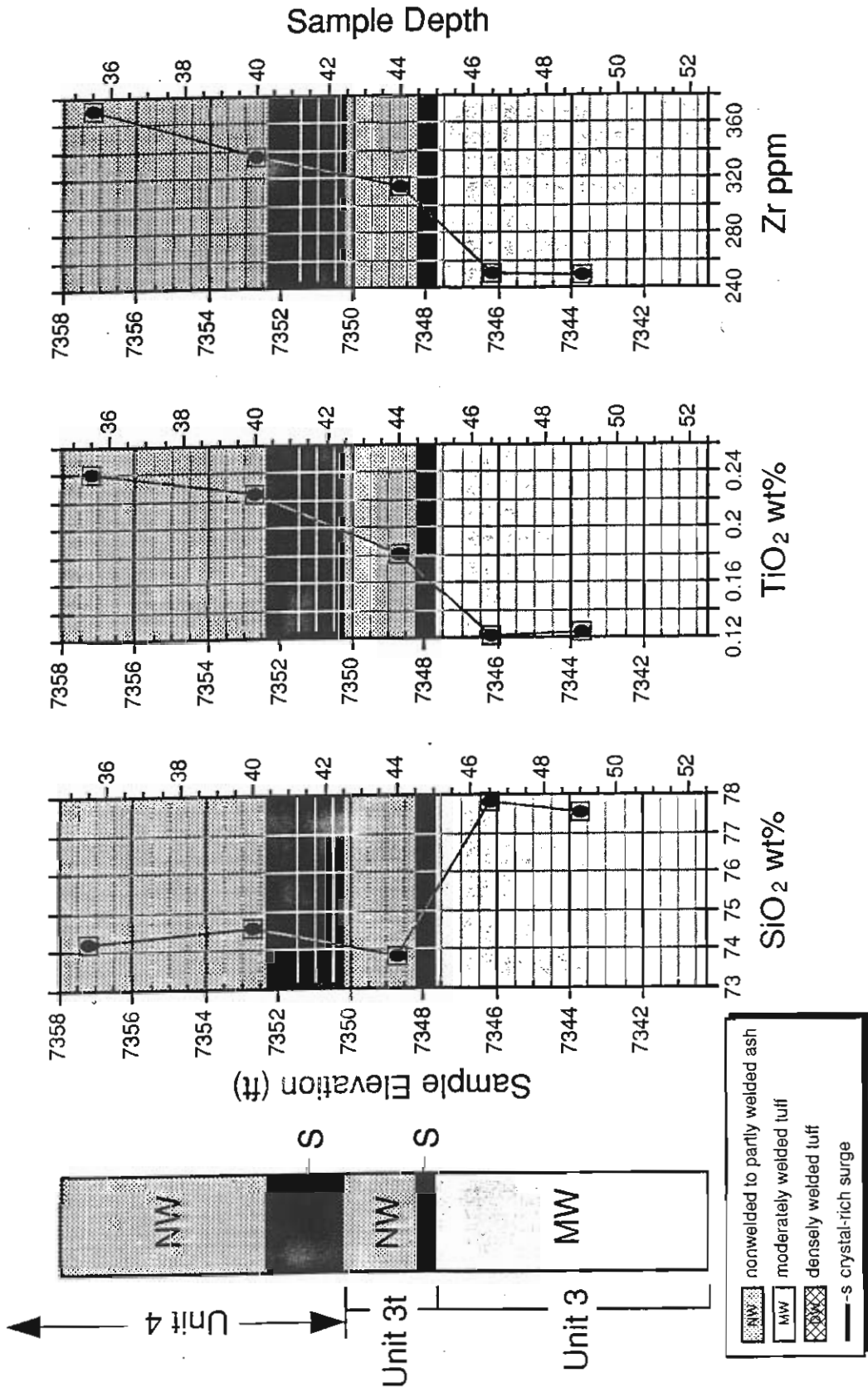


Figure 11. Stratigraphy, welding character, and surge locations compared with SiO₂, TiO₂, and Zr contents for core hole SHB-CMR-8.

SHB-CMR-10

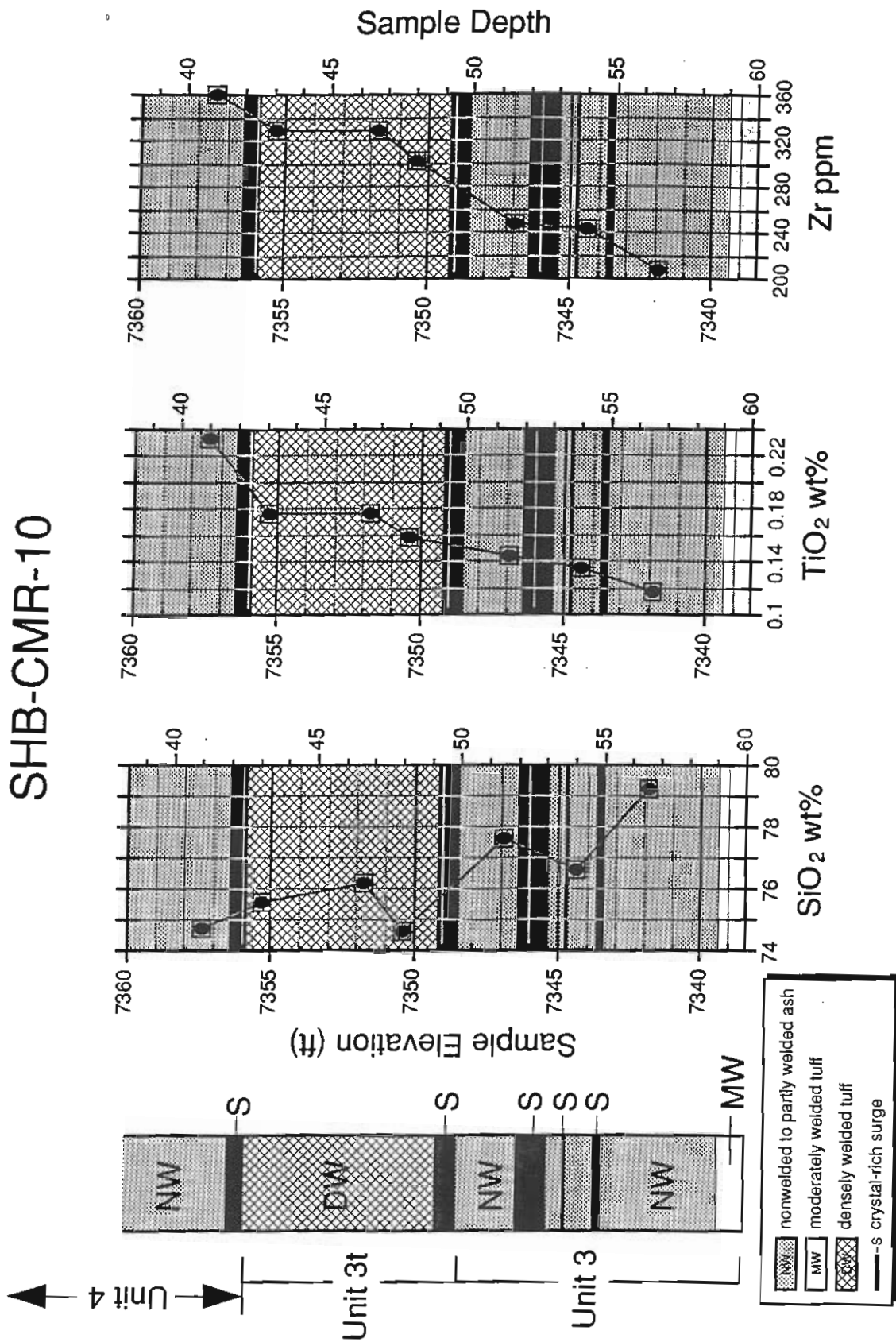


Figure 12. Stratigraphy, welding character, and surge locations compared with SiO₂, TiO₂, and Zr contents for core hole SHB-CMR-10.

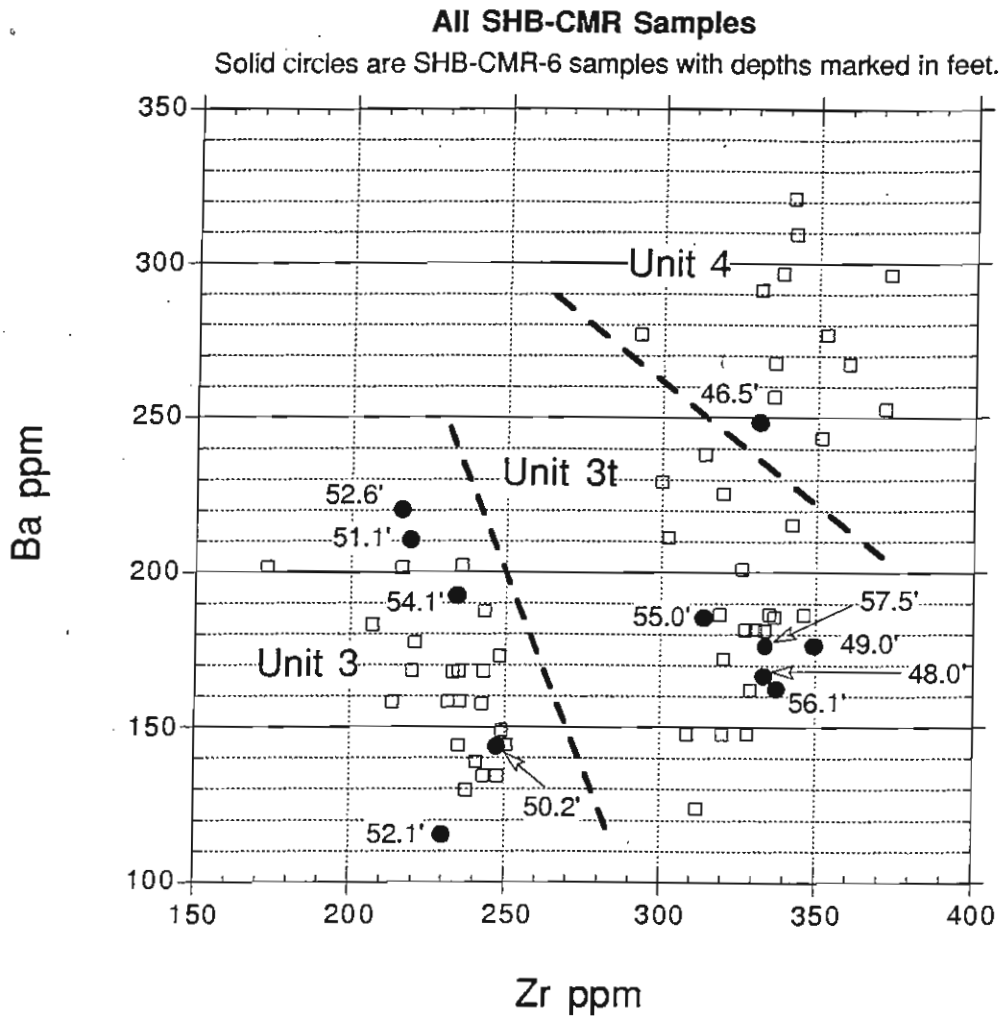


Figure 13. Zr-Ba plot for SHB-CMR samples, with SHB-CMR-6 samples labeled by depth in feet.

A model of the upper surface of Unit 3 was constructed using Surfer-32 software to help visualize the data and the potential for faults in the area of the CMR core holes. The nine core hole locations and elevations of the surface of Unit 3 (Table 2) were used as input. The program uses kriging to interpolate the surface among control points and creates a model of the morphology and attitude of this contact. Figure 14 shows 1-ft contours on the top of the modeled surface of Unit 3. The modeled surface of Unit 3 has an overall strike of approximately N70°W. The dip of this surface is about 1.2° NE in the southwestern portion of the area and steepens to 1.5° NE in the northeast area. The surface increases dip to >2.5° near hole SHB-CMR-6, reflecting the elevation of the faulted contacts observed in SHB-CMR-6 (Section V). Other areas around the CMR building show no evidence of faults disturbing the Unit 3 surface morphology.

Figure 15 displays a detailed solution to the repeated lithologic sequences in hole SHB-CMR-6. Two closely spaced reverse faults cut the core hole to juxtapose Unit 3 against the younger Unit 3t in two places. The combined vertical separation (throw) on these two faults is about 8 ft. Because no fault surfaces, breccias, gouge, alteration, etc., were preserved in the core, the faults are inferred to exist rather than being directly observed. The faults' strikes and dips are not available from the unoriented core. An 80° SE dip is arbitrarily assigned to both faults, and the strikes are assumed to be parallel to each other and to observed air-photolineaments through the region. The resulting strike of the reverse faults is approximately N70°E - S70°W, with a dip of 80°SE.

Figure 16 displays two cross sections drawn through the CMR area. The two faults are illustrated in the figure as a single fault plane for clarity. Figure 16(a) depicts the faults cutting SHB-CMR-6, and Figure 16(b) shows the same faults extending to the southwest to cut Unit 3t between core holes SHB-CMR-2 and SHB-CMR-3. The projection is based on the assigned photolineament orientation as described above. The elevations of the Unit 3 contacts in core holes SHB-CMR-2 and SHB-CMR-3 *permit* the extension of the faults with about 2 ft throw at this locality, but there is no direct evidence of fault extension to this point. There is no other evidence of additional faults beneath the CMR site.

VII. UNCERTAINTY ESTIMATE

Estimates of uncertainties that could affect this study are qualitative, but their consideration reveals that the sources of errors potentially affecting the results are limited. One source of error in depth

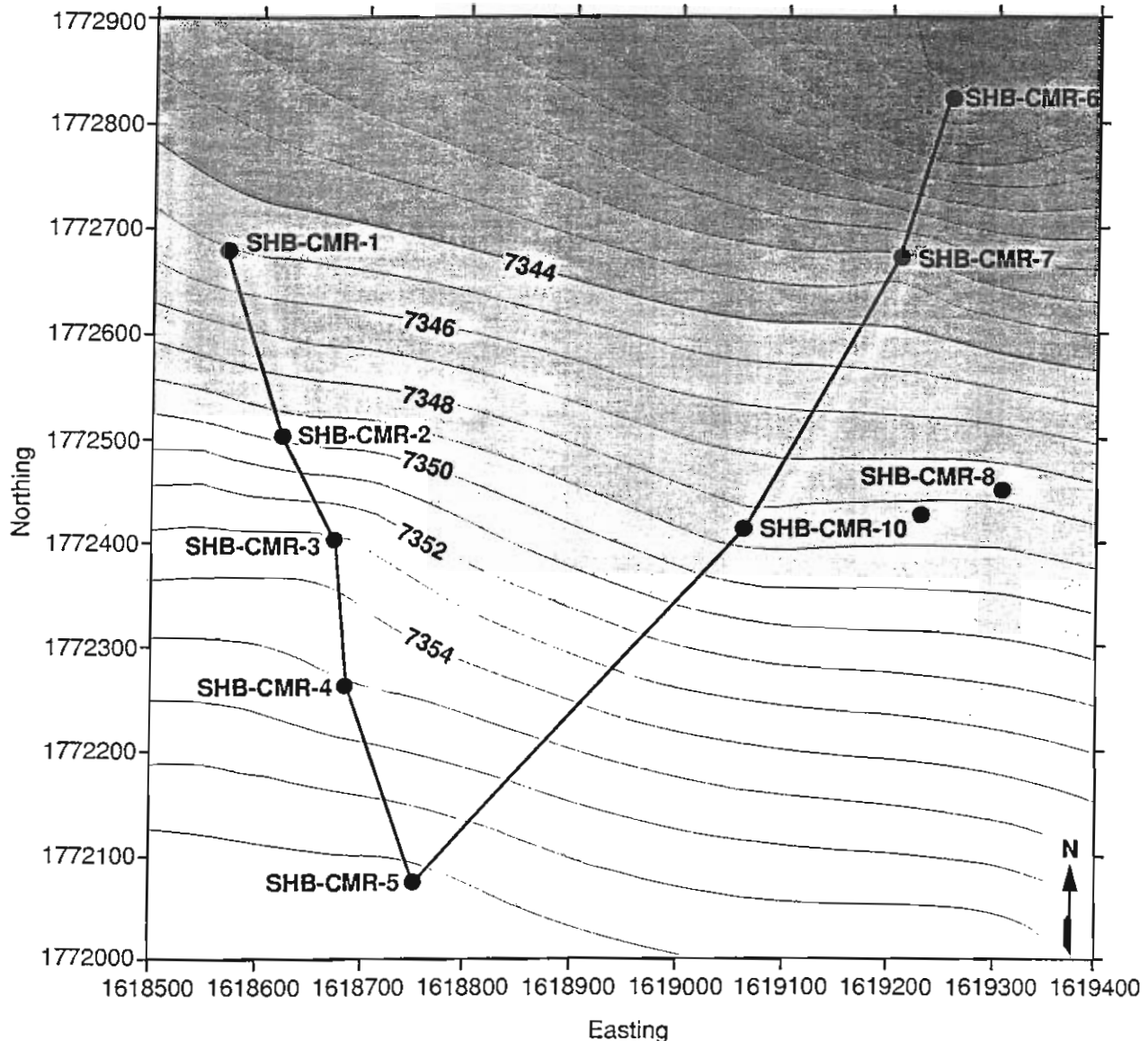


Figure 14. Contour map showing the top surface of Unit 3 in SHB-CMR core holes, as modeled by Surfer 32 software using kriging to interpolate the surface between control points (core holes). The grid is in the State Plane Coordinate System, New Mexico Central Zone, 1983 North American Datum (in feet). The contour interval is 1 ft. The slope of the surface is to the north-northeast. Lines are for the cross sections shown in Figure 16.

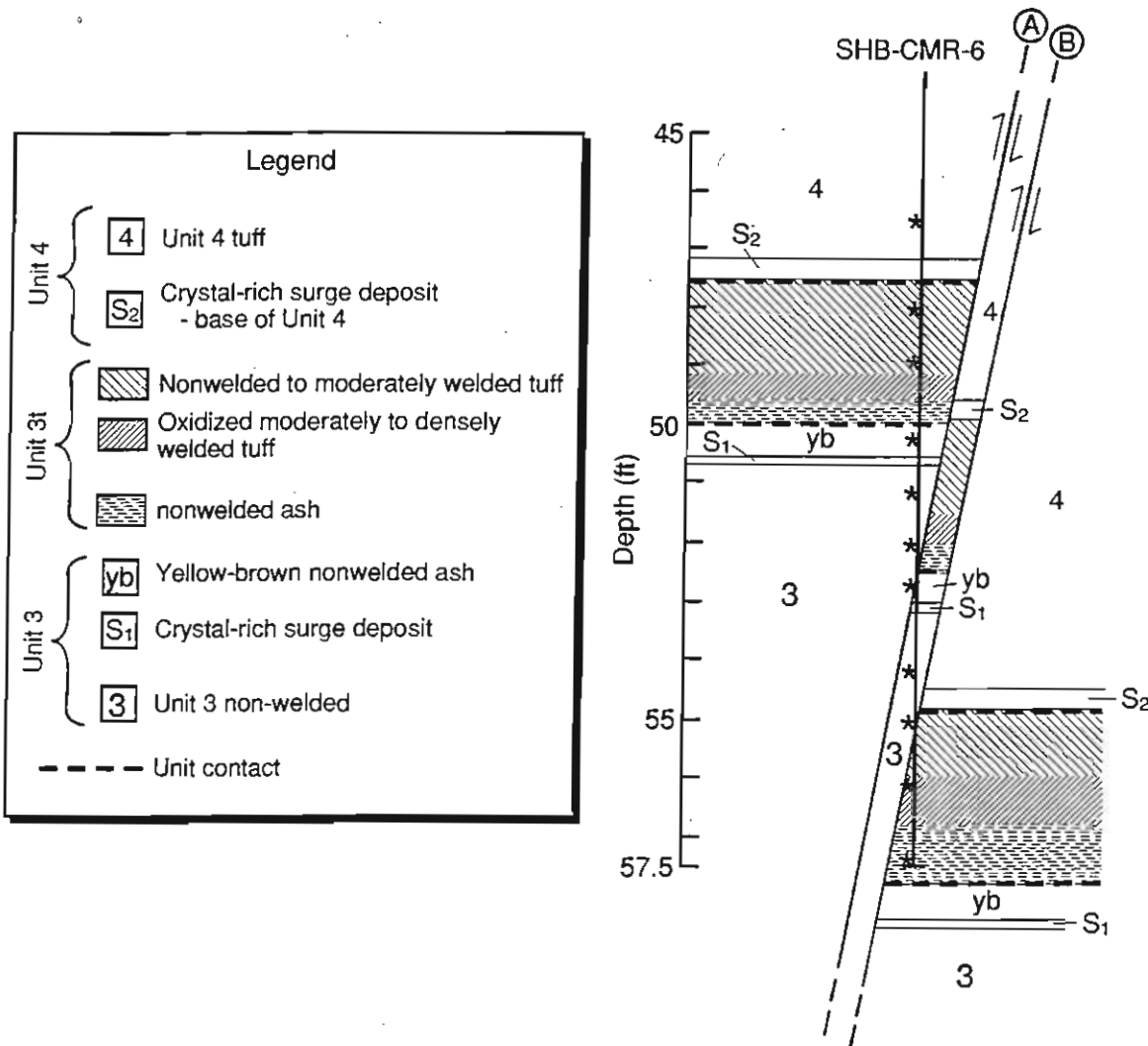


Figure 15. Interpretation of relations observed in core hole SHB-CMR-6 from 45 ft to 57.5 ft (total depths). Two inferred high-angle reverse faults account for the repetition of Unit 3 and Unit 3t lithologic intervals. Fault A has a vertical separation of about 2.5 ft; Fault B has a vertical separation of about 5.5 ft. The total separation is 8 ft. The contacts below the bottom of the core hole are geologically inferred. Asterisks mark the locations of samples for XRF analysis listed in Table 3.

determination is the borehole deviating from the vertical during drilling. The careful drilling and relatively shallow hole depth ensured that each core hole remained at or near its original vertical orientation, hence minimizing this error. The depth intervals from which cores are retrieved during drilling are well known because the number of augers in the ground give an unambiguous measurement of the length of tools in the hole. The coring operation yielded 98% core retrieval, which is excellent recovery in this relatively soft tuff. There are very few "lost" intervals of core. Lithologic logging of this nearly total record makes the mapping unusually complete for this type of investigation. Mapping lithologic types and checking and refining contacts against focused geochemical sampling yield contact elevations accurate to <1 ft in most cases.

Use of a surface-modeling approach with a relatively small data set to infer buried faults is limited by interpretation of changes in dip and strike of marker beds and is mostly grounded in professional judgement. However, core hole SHB-CMR-6 contains physical evidence for faults with a total of 8 ft

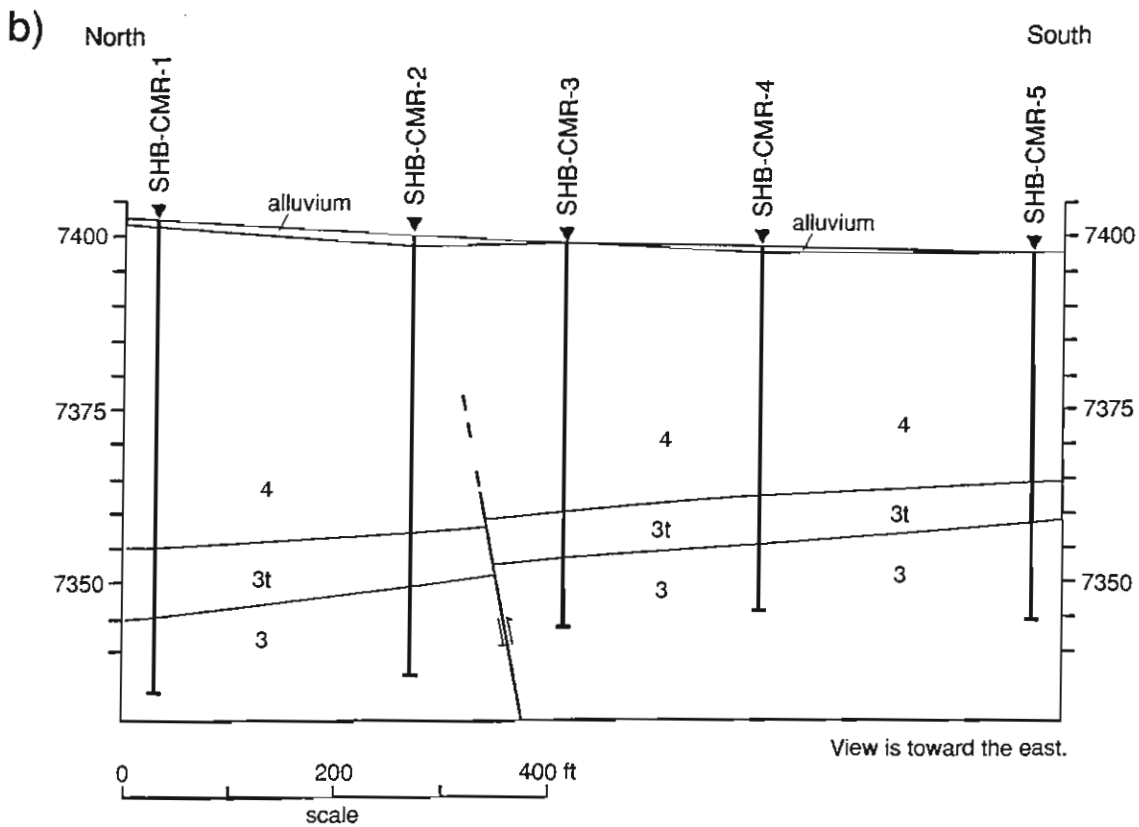
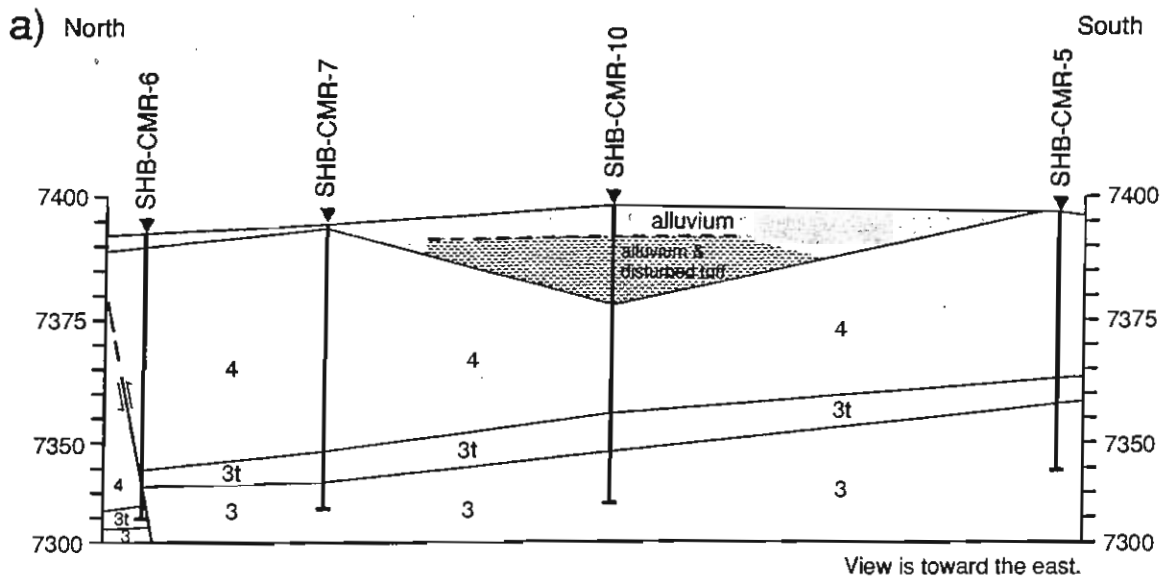


Figure 16. Geologic cross-sections for the lines of section shown on Figure 15. The view is looking east. The two reverse faults cutting SHB-CMR-6 are shown as a single fault for clarity. The faults in SHB-CMR-6 (Figure 16a) are assumed to extend to between SHB-CMR-2 and SHB-CMR-3 (Figure 16b), where the mapped contacts permit up to 2 ft of vertical separation along the fault.

of throw and supports the conclusion that the model is depicting geologic structure rather than a change in dip caused by some depositional process. Also considered were drilling practices or mistakes (for example, hole sloughing or redrilling an interval) that could result in repeated lithologic intervals that are not related to structure in core hole SHB-CMR-6. However, the continuous drilling of the core hole

with hollow-stem augers (no pulling out or backing up) eliminated sloughing or redrilling of tuff that could be incorporated into the core barrel. Similarly, mistakenly reversing which end of the core barrel is "down" during handling in the field does not account for the repeated sections described for this hole.

Southwestward extension of the faults to the region between core holes SHB-CMR-2 and SHB-CMR-3 allows for no more than about 2-ft offset at this locality. This is constrained by the trend of the Unit 3t/3 contact along the line of westernmost holes. This amount is the same as our estimate of the smallest fault that this method can detect.

The final uncertainties involve the assumptions of fault dip (80° SE) and strike ($N70^\circ E - S70^\circ W$). The steep dip is consistent with the great majority of joints and faults observed within the Bandelier Tuff on the Pajarito Plateau (for example, Vaniman and Chipera, 1995; Wohletz, 1995). The fault strike is consistent with faults mapped nearby by Gardner et al. (1998) and with lineaments observed on early air-photos of the CMR site. These circumstances provide reasonable constraints on the faults' probable orientation, given the lack of any orientation directly observed in the cores.

VIII. CONCLUSIONS

Two small faults are present in the subsurface near the northern edge of the CMR building at TA-3, LANL. These reverse faults, detected in one core hole, have a combined vertical separation of about 8 ft. When considered with the marker beds observed in the other core holes, the data allow for extension of the fault toward the southwest beneath the CMR building to the area between holes SHB-CMR-2 and SHB-CMR-3, where no more than 2 ft of throw can be accommodated. No other faults were detected or inferred to exist beneath the CMR building.

The faults in SHB-CMR-6 are probably related to the southern extension of the Rendija Canyon fault zone. The north-south trending Rendija Canyon fault has been shown by Gardner et al. (1998) to change style and orientation to smaller southwest-northeast trending fault splays with decreasing offset toward the southwest. Diminishing displacement along the fault and lack of any geomorphological expression indicate that the fault is dying (i.e., diminishing to zero offset) toward the southwest, at least in the 1.22-Ma-old, near-surface rocks of the Tshirege Member of the Bandelier Tuff. Similar reverse faults and other normal faults associated with the Rendija Canyon fault have been mapped in exposures at the Los Alamos County landfill, although it is doubtful that any of these faults are continuous with those in hole SHB-CMR-6. Other subsurface faults could be undetected in the vicinity of the CMR building, but the data constrain the throw on such faults to <2 ft for the zone beneath the building.

The CMR drilling results provide a bound for probabilistic seismic hazard analysis of potential surface rupture at TA-3 and beneath the CMR building (Olig et al., 1998). The small reverse faults, although a possible extension of the Rendija Canyon fault zone, have an opposite sense of displacement to the main trace of the Rendija Canyon fault further north. They are examples of distributed or subsidiary fault splays related to the southwestern terminus of the Rendija Canyon fault, a fault that has as much as an order of magnitude more displacement on Bandelier Tuff in northern Los Alamos County.

IX. ACKNOWLEDGMENTS

The Nuclear Weapons Technologies Programs office, T. J. Trapp, Jim Holt, Chief of Staff at NWT, and Carolyn Zerkle (NMT) arranged funding for the CMR subsurface investigation. Scott Dick (NMT-13),

Larry Haynes (NMT-8), and Bob Pruner (NMT-13) lead us through the work authorization process for working at the CMR facility. Bill Bell and Grady Rose of the Department of Energy provided guidance and safety oversight before and during the drilling program. Larry Goen (ESA) and Doug Volkman (FSS) provided support and program management for the Seismic Hazards Program. Emily Kluk and Rick Warren (EES-1) performed the XRF analyses in the EES-1 group analytical facilities. Technical review of this report was done by David Vaniman (EES-1). Anthony Garcia, Alexis Lavine, and Lanny Piotrowski provided illustrations. Lanny also did the compositing of the final manuscript for publication. This work was funded by the U.S. Department of Energy. All of this support is greatly appreciated.

X. REFERENCES

- Broxton, D. E., and Reneau, S. L., 1995, Stratigraphic nomenclature of the Bandelier Tuff for the Environmental Restoration Project at Los Alamos National Laboratory; Los Alamos National Laboratory report LA-13010-MS.
- Criss, J., 1980, Fundamental parameters calculations on a laboratory microcomputer, *Advances in X-Ray Analysis* **23**, pp. 93-97.
- Dransfield, B. J., and Gardner, J. N., 1985, Subsurface geology of the Pajarito Plateau, Espanola Basin, New Mexico; Los Alamos National Laboratory report LA-10455-MS.
- Gardner, J. N., and Goff, F., 1984, Potassium-argon dates from the Jemez volcanic field: Implications for tectonic activity in the north-central Rio Grande rift; *New Mexico Geological Society Guidebook* **35**, pp. 75-81.
- Gardner, J. N., Goff, F., Garcia, S., and Hagan, R. C., 1986, Stratigraphic relations and lithologic variations in the Jemez volcanic field, New Mexico; *Journal of Geophysical Research* **91**, pp. 1763-1778.
- Gardner, J. N., and House, L., 1987, Seismic hazards investigations at Los Alamos National Laboratory, 1984 to 1985; Los Alamos National Laboratory report LA-11072-MS.
- Gardner, J. N., Lavine, A., Vaniman, D., and WoldeGabriel, G., 1998, High-precision mapping to evaluate the potential for seismic surface rupture at TA-55, Los Alamos National Laboratory; Los Alamos National Laboratory report LA-13456-MS.
- Geological Society of America, 1980, *Rock-Color Chart*; Geological Society of America, Boulder, Colorado.
- Goff, S., 1986, Curatorial policy guidelines and procedures for the Continental Scientific Drilling Program; Los Alamos National Laboratory report LA-10542-OBES, Los Alamos, NM.
- Griggs, R. L., 1964, *Geology and groundwater resources of the Los Alamos area, New Mexico*; U.S. Geological Survey Water-Supply Paper 1753, 107 p.
- Heiken, G., Goff, F., Stix, J., Tamanyu, S., Shafiqullah, M., Garcia, S., and Hagan, R., 1986, Intracaldera volcanic activity, Toledo caldera and embayment, Jemez Mountains, New Mexico, *Journal of Geophysical Research* **91**, pp. 1799-1815.

- Izett, G. A., and Obradovich, J. D., 1994, $^{40}\text{Ar}/^{39}\text{Ar}$ -age constraints for the Jaramillo Normal Subchron and the Matuyama-Brunhes geomagnetic boundary; *Journal of Geophysical Research* **99**, pp. 2925-2934.
- Krier, D., Caporuscio, F., Lavine, A., and Gardner, J., 1998, Stratigraphy and geologic structure at the SCC and NISC building sites, Technical Area 3, Los Alamos National Laboratory, New Mexico; Los Alamos National Laboratory report LA-13507-MS.
- Lavine, A., Heiken, G. H., and Stix, J., 1997, Stratigraphy and distribution of Cerro Toledo tephra and volcaniclastic sediments beneath the Pajarito Plateau, Jemez Mountains, New Mexico (abstract); *New Mexico Geology* **19**.
- Olig, S., Youngs, R., and Wong, I., 1998, Preliminary probabilistic seismic hazard analysis for surface fault displacement at TA-3, Los Alamos National Laboratory; Woodward-Clyde Federal Services.
- Smith, R. L., and Bailey, R. A., 1966, The Bandelier Tuff: a study of ash-flow eruption cycles and zoned magma chambers; *Bulletin of Volcanology* **29**, pp. 83-104.
- Smith, R. L., Bailey, R. A., and Ross, C. S., 1970, Geologic map of the Jemez Mountains, New Mexico, U.S. Geological Survey Miscellaneous Geological Investigations Map I-571, 1:125,000 scale.
- Stimac, J. A., Broxton, D. E., Kluk, E. C., and Chipera, S. J., Preliminary stratigraphy of tuffs from borehole 49-2-700-1 at Technical Area 49, Los Alamos National Laboratory, New Mexico (in preparation).
- Vaniman, D. and Chipera, S., 1995, Mesa penetrating fractures, fracture mineralogy, and projected fault traces at Pajarito Mesa, *in* Geological Site Characterization for the Proposed Mixed Waste Disposal Facility, Los Alamos National Laboratory, Los Alamos National Laboratory report LA-13089-MS, S. Reneau and R. Raymond, Jr., editors, pp. 71-86.
- Warren, R. G., McDonald, E. V., and Rytli, R. T., 1998, Baseline geochemistry of soil and bedrock, Tshirege Member of the Bandelier Tuff at MDA P, Los Alamos National Laboratory report LA-13330-MS.
- Wohletz, K., 1995, Measurement and analysis of rock fractures in the Tshirege Member of the Bandelier Tuff along Los Alamos Canyon adjacent to Technical Area 21, *in* Earth Science Investigations for Environmental Restoration—Los Alamos National Laboratory Technical Area 21, Los Alamos National Laboratory report LA-12934-MS, D. Broxton and P. Eller, editors, pp. 19-32.
- Wong, I., Kelson, K., Olig, S., Kolbe, T., Hemphill-Haley, M., Bott, J., Green, R., Kanakari, H., Sawyer, J., Silva, W., Stark, C., Haraden, C., Fenton, C., Unruh, J., Gardner, J., Reneau, S., and House, L., 1995, Seismic hazards evaluation of the Los Alamos National Laboratory; report prepared for Los Alamos National Laboratory by Woodward-Clyde Federal Services, Oakland, California.